Chapter 9
Double-Diffusive Convection

In this chapter we turn our attention to processes of combined (simultaneous) heat and mass transfer that are driven by buoyancy. The density gradients that provide the driving buoyancy force are induced by the combined effects of temperature and species concentration nonuniformities present in the fluid-saturated medium. The present chapter is guided by the review of Trevisan and Bejan (1990), which began by showing that the conservation statements for mass, momentum, energy, and chemical species are the equations that have been presented here in Chaps. 1–3. In particular the material in Sect. 3.3 is relevant. The new feature is that beginning with Eq. (3.26) the buoyancy effect in the momentum equation is represented by two terms, one due to temperature gradients and the other to concentration gradients. Useful review articles on double-diffusive convection include those by Mojtabi and Charrier-Mojtabi (2000, 2005), Mamou (2002b), Diersch and Kolditz (2002), and Mojtabi et al. (2015).

9.1 Vertical Heat and Mass Transfer

9.1.1 Horton-Rogers-Lapwood Problem

The interesting effects in double-diffusive (or thermohaline, if heat and salt are involved) convection arise from the fact that heat diffuses more rapidly than a dissolved substance. Whereas a stratified layer involving a single-component fluid is stable if the density decreases upward, a similar layer involving a fluid consisting of two components, which can diffuse relative to each other, may be dynamically unstable. If a fluid packet of such a mixture is displaced vertically, it loses any excess heat more rapidly than any excess solute. The resulting buoyancy may act to either increase the displacement of the particle, and thus cause monotonic instability, or reverse the direction of the displacement and so cause oscillatory

D.A. Nield, A. Bejan, *Convection in Porous Media*,
DOI 10.1007/978-3-319-49562-0_9

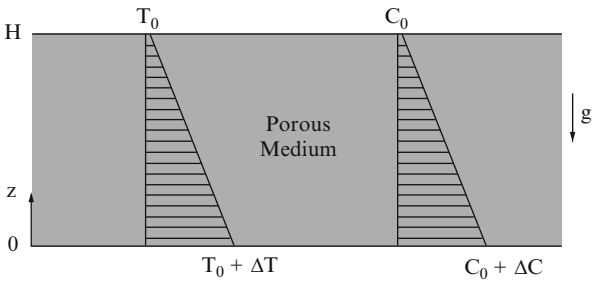

Fig. 9.1 Infinite horizontal porous layer with linear distributions of temperature and concentration

instability, depending on whether the solute gradient is destabilizing and the temperature gradient is stabilizing or vice versa.

The double-diffusive generalization of the Horton-Rogers-Lapwood problem was studied by Nield (1968). In terms of the temperature T and the concentration C, we suppose that the density of the mixture is given by Eq. (3.26),

$$\rho_{\mathrm{f}} = \rho_0[1 - \beta(T - T_0) - \beta_{\mathrm{C}}(C - C_0)]. \tag{9.1}$$

In this equation $\beta_{\mathrm{C}} = -\rho_{\mathrm{f}}{}^{-1}\partial\rho_{\mathrm{f}}/\partial C$ is a concentration expansion coefficient analogous to the thermal expansion coefficient $\beta = -\rho_{\mathrm{f}}{}^{-1}\partial\rho_{\mathrm{f}}/\partial T$. We assume that β_{C} and β are constants. In most practical situations β_{C} will have a negative value.

As shown in Fig. 9.1, we suppose that the imposed conditions on C are

$$C = C_0 + \Delta C \text{ at } \quad z = 0 \text{ and } C = C_0 \text{ at } \quad z = H. \tag{9.2}$$

The conservation equation for chemical species is

$$\varphi\frac{\partial C}{\partial t} + \mathbf{v}\cdot\nabla C = D_{\mathrm{m}}\nabla^2 C \tag{9.3}$$

and the steady-state distribution is linear:

$$C_{\mathrm{s}} = C_0 + \Delta C\left(1 - \frac{z}{H}\right). \tag{9.4}$$

Proceeding as in Sect. 6.2, choosing ΔC as concentration scale and putting $\widehat{C} = C'/\Delta C$, and writing

$$\widehat{C} = \gamma(z)\exp\left(\widehat{s}t + il\widehat{x} + im\widehat{y}\right), \tag{9.5}$$

we obtain

$$\left[\mathrm{Le}^{-1}\left(D^2 - \alpha^2\right) - \frac{\varphi}{\sigma}s\right]\gamma = -W. \tag{9.6}$$

In place of Eq. (6.23) we now have, if γ_a is negligible,

$$\left(D^2 - \alpha^2\right)W = -\alpha^2 \mathrm{Ra}(\theta + N\gamma), \tag{9.7}$$

while Eq. (6.22) remains unchanged, namely

$$\left(D^2 - \alpha^2 - s\right)\theta = -W. \tag{9.8}$$

The nondimensional parameters that have appeared are the Rayleigh and Lewis numbers

$$\mathrm{Ra} = \frac{g\beta KH\Delta T}{\nu\alpha_m}, \quad \mathrm{Le} = \frac{\alpha_m}{D_m}, \tag{9.9}$$

and the buoyancy ratio

$$N = \frac{\beta_C \Delta C}{\beta \Delta T}. \tag{9.10}$$

If both boundaries are impermeable, isothermal (conducting), and isosolutal (constant C), then Eqs. (9.6)–(9.8) must be solved subject to

$$W = \theta = \gamma = 0 \text{ at } \quad \widehat{z} = 0 \text{ and } \widehat{z} = 1. \tag{9.11}$$

Solutions of the form

$$(W, \theta, \gamma) = (W_0, \theta_0, \gamma_0) \sin j\pi\widehat{z} \tag{9.12}$$

are possible if

$$J(J + s)(J + \Phi_s) = \mathrm{Ra}\,\alpha^2(J + \Phi_s) + \mathrm{Ra_D}\alpha^2(J + s), \tag{9.13}$$

where

$$J = j^2\pi^2 + \alpha^2, \quad \Phi = \frac{\varphi}{\sigma}\mathrm{Le}, \quad \mathrm{Ra_D} = NLeRa = \frac{g\beta_C KH\Delta C}{\nu D_m}. \tag{9.14}$$

At marginal stability, $s = i\omega$ where ω is real, and the real and imaginary parts of Eq. (9.13) yield

$$J^2 - \Phi\omega^2 = (\mathrm{Ra} + \mathrm{Ra}_D)\alpha^2, \tag{9.15}$$

$$\omega\left[J^2(1 + \Phi) - (\Phi Ra + \mathrm{Ra}_D)\alpha^2\right] = 0. \tag{9.16}$$

This system implies either $\omega = 0$ and

$$\mathrm{Ra} + \mathrm{Ra_D} = \frac{J^2}{\alpha^2}, \tag{9.17}$$

or

$$\Phi Ra + \mathrm{Ra_D} = (1 + \Phi)\frac{J^2}{\alpha^2}, \tag{9.18}$$

and

$$\Phi\frac{\omega^2}{\alpha^2} = \frac{J^2}{\alpha^2} - (\mathrm{Ra} + \mathrm{Ra_D}). \tag{9.19}$$

Since J^2/α^2 has the minimum value $4\pi^2$, attained when $j = 1$ and $\alpha = \pi$, we conclude that the region of stability in the (Ra, $\mathrm{Ra_D}$) plane is bounded by the lines

$$\mathrm{Ra} + \mathrm{Ra_D} = 4\pi^2, \tag{9.20}$$

$$\Phi Ra + \mathrm{Ra_D} = 4\pi^2(1 + \Phi), \tag{9.21}$$

Equation (9.20) represents the boundary for monotonic or stationary instability, and Eq. (9.21) is the boundary for oscillatory instability with frequency ω given by

$$\Phi\frac{\omega^2}{\pi^2} = 4\pi^2 - (\mathrm{Ra} + \mathrm{Ra_D}). \tag{9.22}$$

Clearly the right-hand side of Eq. (9.22) must be nonnegative in order to yield a real value for ω.

If $\Phi = 1$, then the lines (9.20) and (9.21) are parallel, with the former being nearer the origin. Otherwise they intersect at

$$\mathrm{Ra} = \frac{4\pi^2\Phi}{\Phi - 1}, \quad \mathrm{Ra_D} = \frac{4\pi^2}{1 - \Phi}, \tag{9.23}$$

Illustrated in Fig. 9.2 is the case $\Phi > 1$, which corresponds to $\mathrm{Le} > \sigma/\varphi$.

The cases of other combinations of boundary conditions can be treated in a similar manner. If the boundary conditions on the temperature perturbation θ are formally identical with those of the solute concentration perturbation γ, then the monotonic instability boundary is a straight line:

$$\mathrm{Ra} + \mathrm{Ra_D} = \mathrm{Ra_c}. \tag{9.24}$$

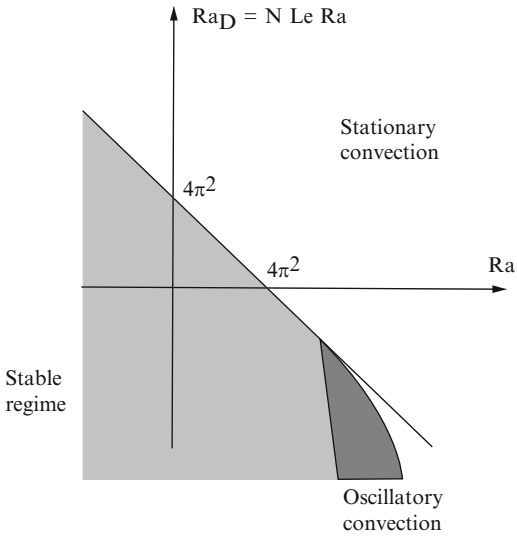

Fig. 9.2 The stability and instability domains for double-diffusive convection in a horizontal porous layer

One can interpret Ra as the ratio of the rate of release of thermal energy to the rate of viscous dissipation of energy and a similar interpretation applies to Ra_D. When the thermal and solutal boundary conditions are formally identical, the eigenfunctions of the purely thermal and purely solutal problems are identical, and consequently the thermal and solutal effects are additive. When the two sets of boundary conditions are different, the coupling between the thermal and solutal agencies is less than perfect and one can expect that the monotonic instability boundary will be concave toward the origin, since then $Ra + Ra_D \geq Ra_c$ with equality occurring only when $Ra = 0$ or $Ra_D = 0$.

When Ra and Ra_D are both positive the double-diffusive situation is qualitatively similar to the single-diffusive one. When Ra and Ra_D have opposite signs there appear interesting new phenomena: multiple steady- and unsteady-state solutions, subcritical flows, periodic or chaotic oscillatory flows, traveling waves in relatively large aspect ratio enclosures, and axisymmetric flow structures. Such phenomena arise generally because the different diffusivities lead to different time scales for the heat and solute transfer. But similar phenomena can arise even when the thermal and solutal diffusivities are nearly equal because of the factor φ/σ (often called the normalized porosity). This is because heat is transferred through both the fluid and solid phases but the solute is necessarily transported through the fluid phase only since the porous matrix material is typically impermeable.

Experiments with a Hele-Shaw cell by Cooper et al. (1997, 2001) and Pringle et al. (2002) yielded results in agreement with the theory.

In his study of gas/vapor mixtures, Davidson (1986) allowed for the temperature dependence of mixture properties. Murty et al. (1994b) studied numerically the stability of thermohaline convection in a rectangular box. Nield (1995b) pointed out that they had overlooked the possibility of oscillatory instability.

Some asymptotic formulas were presented by Rosenberg and Spera (1992). Forsyth and Simpson (1991) presented a two-phase, two-component model.

The special case of isoflux boundary conditions was discussed by Nield and Kuznetsov (2016c). In this case convection occurs at a very small wavenumber and oscillatory convection is inhibited.

9.1.2 Nonlinear Initial Profiles

Since the diffusion time for a solute is relatively large, it is particularly appropriate to discuss the case when the concentration profile is nonlinear, the basic concentration distribution being given by

$$C_s = C_0 + \Delta C[1 - F_c(\hat{z})]. \tag{9.25}$$

The corresponding nondimensional concentration gradient is $f_c(\hat{z}) = F_c'(\hat{z})$, and satisfies $< f_c'(\hat{z}) >= 1$, where the angle brackets denote the vertical average. Then, in place of Eq. (9.6) one now has

$$\left[\mathrm{Le}^{-1}\left(D^2 - \alpha^2\right) - \frac{\varphi}{\sigma}s\right]\gamma = -f_c(\hat{z})W. \tag{9.26}$$

In the case of impermeable conducting boundaries, the Galerkin method of solution (trial functions of the form $\sin l\pi\hat{z}$ with $l = 1, 2, \ldots$) gives as the first approximation to the stability boundary for monotonic instability,

$$\mathrm{Ra} + 2\mathrm{Ra_D} < f_c(\hat{z})\sin^2\pi^2\hat{z} >= 4\pi^2. \tag{9.27}$$

For example, for the cosine profile with $F_c(\hat{z}) = (1 - \cos\pi\hat{z})/2$, and hence with $f_c = (\pi/2)\sin\pi\hat{z}$, we get

$$\mathrm{Ra} + \frac{4}{3}\mathrm{Ra_D} = 4\pi^2. \tag{9.28}$$

Similarly, for the step-function concentration, with $F_c(\hat{z}) = 0$ for $0 \le \hat{z} < ½$ and $F_c(\hat{z}) = 1$ for $½ < \hat{z} \le 1$, so that $f_c(\hat{z}) = \delta(\hat{z} - ½)$, we have

$$\mathrm{Ra} + \mathrm{Ra_D} = 4\pi^2. \tag{9.29}$$

The approximation leading to this result requires that $|\mathrm{Ra_D}|$ be small.

9.1.3 Finite-Amplitude Effects

Experiments in viscous fluids have shown that monotonic instability, associated with warm salty water above cool fresh water, appears in the form of "fingers" that grow downward from the upper part of the layer. More generally, fingering occurs

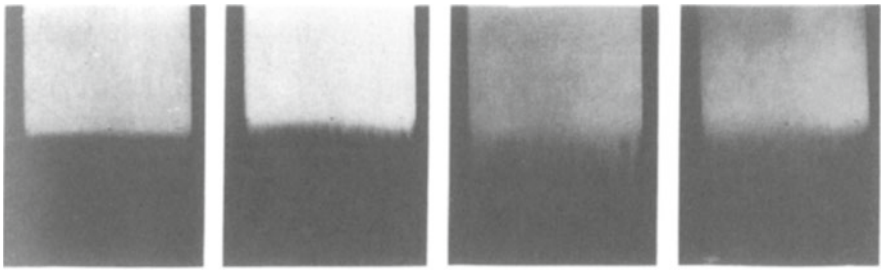

Fig. 9.3 A series of pictures of finger growth. Dyed sugar solution (*light color*) overlies heavier salt solution (Imhoff and Green 1988, with permission from Cambridge University Press)

when the faster diffusing component is stabilizing and the slower diffusing component is destabilizing. This situation is referred to as the fingering regime. On the other hand, oscillatory instability, associated with warm salty water below cool fresh water, gives rise to a series of convecting layers that form in turn, each on top of its predecessor. This situation is referred to as the diffusive regime.

In the case of a porous medium the questions are whether the fingers form fast enough before they are destroyed by dispersive effects and whether their width is large enough compared to the grain size for Darcy's law to be applicable. Following earlier work by Taunton et al. (1972), these questions were examined by Green (1984), who, on the basis of his detailed analysis, predicted that fluxes associated with double-diffusive fingering may well be important but horizontal dispersion may limit the vertical coherence of the fingers. In their visualization and flux experiments using a sand-tank model and a salt-sugar system, Imhoff and Green (1988) found that fingering did indeed occur but it was quite unsteady, in contrast to the quasisteady fingering observed in a viscous fluid (Fig. 9.3). Despite the unsteadiness, good agreement was attained with the theoretical predictions. Imhoff and Green (1988) concluded that fingering could play a major role in the vertical transport of contaminants in groundwater.

(It should be noted that these fingers are distinct from those studied extensively by Wooding (1959, 1960a, b, 1962a, b, 1964, 1969). The spacing of the double-diffusive fingers is determined by the critical wavenumber determined by the Rayleigh–Bćnard instability theory while the monodiffusive fingers investigated by Wooding arise from Rayleigh–Taylor instability and the spacing is on a smaller length scale. In this case the hydrological situation can be complex (Xie et al. 2012).)

That layered double-diffusive convection is possible in a porous medium was shown by Griffiths (1981). His experiments with a two-layer convecting system in a Hele–Shaw cell and a porous medium of glass spheres indicated that a thin "diffusive" interface is maintained against diffusive thickening, despite the lack of inertial forces. The solute and thermal buoyancy fluxes are approximately in the ratio $r = \varphi \, \mathrm{Le}^{-1/2}$. Griffiths explained the behavior of the heat flux in terms of a coupling between purely thermal convection within each convecting layer and

diffusion through the density interface. Further experiments in a Hele–Shaw cell by Pringle and Glass (2002) explored the influence of concentration at a fixed buoyancy ratio.

Rudraiah et al. (1982a) applied nonlinear stability analysis to the case of a porous layer with impermeable, isothermal, and isosolutal boundaries. They reported Nusselt and Sherwood numbers for Ra values up to 300 and Ra_D values up to 70. Their results show that finite-amplitude instability is possible at subcritical values of Ra.

Brand and Steinberg (1983a, b) and Brand et al. (1983) have obtained amplitude equations appropriate for the onset of monotonic instability and oscillatory instability and also for points in the vicinity of the lines of monotonic and oscillatory instability. Brand et al. (1983) found an experimentally feasible example of a codimensional-two bifurcation (an intersection of monotonic and oscillatory instability boundaries). Brand and Steinberg (1983b) predicted that the Nusselt number and also the "Froude" (Sherwood) number should oscillate with a frequency twice that of the temperature and concentration fields. Small-amplitude nonlinear solutions in the form of standing and traveling waves and the transition to finite-amplitude overturning convection, as predicted by bifurcation theory, were studied by Knobloch (1986). Rehberg and Ahlers (1985) reported heat transfer measurements in a normal-fluid He^3–He^4 mixture in a porous medium. They found a bifurcation to steady or oscillatory flow, depending on the mean temperature, in accordance with theoretical predictions.

Murray and Chen (1989) have extended the linear stability theory, taking into account effects of temperature-dependent viscosity and volumetric expansion coefficients and a nonlinear basic salinity profile. They also performed experiments with glass beads in a box with rigid isothermal lower and upper boundaries. These provide a linear basic-state temperature profile but only allow a nonlinear and time-dependent basic-state salinity profile. With distilled water as the fluid, the convection pattern consisted of two-dimensional rolls with axes parallel to the shorter side. In the presence of stabilizing salinity gradients, the onset of convection was marked by a dramatic increase in heat flux at a critical temperature difference ΔT. The convection pattern was three-dimensional, whereas two-dimensional rolls are observed for single-component convection in the same apparatus. When ΔT was then reduced from supercritical to subcritical values the heat flux curve completed a hysteresis loop.

For the case of uniform flux boundary conditions, Mamou et al. (1994) have obtained both analytical asymptotic and numerical solutions, the latter for various aspect ratios of a rectangular box. Both uniform flux and uniform temperature boundary conditions were considered by Mamou and Vasseur (1999) in their linear and nonlinear stability, analytical, and numerical studies. They identified four regimes dependent on the governing parameters: stable diffusive, subcritical convective, oscillatory, and augmenting direct regimes. Their results indicated that steady convection can arise at Rayleigh numbers below the supercritical value for linear stability, indicating the development of subcritical flows. They also demonstrated that in the overstable regime multiple solutions can exist. Also, their

numerical results indicate the possible occurrence of traveling waves in an infinite horizontal enclosure.

A nonlinear stability analysis using the Lyapunov direct method was reported by Lombardo et al. (2001) and Lombardo and Mulone (2002). A numerical study of the governing and perturbation equations, with emphasis on the transition from steady to oscillatory flows and with an acceleration parameter taken into consideration, was conducted by Mamou (2003). The numerical and analytic study by Mbaye and Bilgen (2001) demonstrated the existence of subcritical oscillatory instabilities. The numerical study by Mohamad et al. (2004) for convection in a rectangular enclosure examined the effect of varying the lateral aspect ratio. Schoofs et al. (1999) discussed chaotic thermohaline convection in the context of low-porosity hydrothermal systems. Schoofs and Spera (2003) in their numerical study observed that increasing the ratio of chemical buoyancy to thermal buoyancy, with the latter kept fixed, led to a transition from steady to chaotic convection with a stable limit cycle appearing at the transition. The dynamics of the chaotic flow is characterized by transitions between layered and nonlayered patterns as a result of the spontaneous formation and disappearance of gravitationally stable interfaces. These interfaces temporally divide the domain in layers of distinct solute concentration and lead to a significant reduction of kinetic energy and vertical heat and solute fluxes. A scale analysis, supported by numerical calculations, was presented by Bourich et al. (2004c) for the case of bottom heating and a horizontal solutal gradient. The case of mixed boundary conditions (constant temperature and constant mass flux, or vice versa) was studied numerically by Mahidjiba et al. (2000a). They found that when the thermal and solute effects are opposing the convection patterns differ markedly from the classic Bénard ones.

Mulone and Straughan described an operative method to obtain necessary and sufficient stability conditions. An extension to the case of systems with spatially dependent coefficients (such as the case of a concentration based internal heat source) was made by Hill and Malashetty (2012). Falsaperla et al. (2012) studied rotating porous media under general boundary conditions. Peterson et al. (2010) performed a multiresolution simulation of double-diffusive convection. Umla et al. (2010) examined roll convection of binary fluid mixtures. Global stability for penetrative convection was studied by Hill (2008). A differential equation approach to obtain global stability for radiation-induced convection was introduced by Hill (2009). Lo Jacono et al. (2010) studied the origin and properties of time-independent spatially localized convection, computing using numerical continuation different types of single and multipulse states. Rionero (2012d) re-examined global nonlinear stability in double-diffusive convection in the light of hidden symmetries. Diaz and Brevdo (2011, 2012) examined the absolute/convective instability dichotomy at the onset of convection with either horizontal or vertical solutal and inclined thermal gradients and with horizontal throughflow.

The effect of form drag on nonlinear convection and Hopf bifurcation (that characterizes the transition from steady to unsteady convection) was studied by Rebhi et al. (2016a, b). They found that hysteresis could be induced by the form drag, and that a bistability phenomenon arose when the subcritical instability threshold was close to the threshold for supercritical instability.

9.1.4 Soret and Dufour Cross-Diffusion Effects

In the case of steep temperature gradients the cross coupling between thermal diffusion and solutal diffusion may no longer be negligible. The tendency of a solute to diffuse under the influence of a temperature gradient is known as the Soret effect.

In its simplest expression, the conservation equation for C now becomes

$$\varphi \frac{\partial C}{\partial t} + v \cdot \nabla C = D_{\mathrm{m}} \nabla^2 C + D_{\mathrm{CT}} \nabla^2 T, \tag{9.30}$$

where the Soret coefficient D_{CT} is treatable as a constant. If the Soret parameter S is defined as

$$S = -\frac{\beta_{\mathrm{C}} D_{\mathrm{CT}}}{\beta D_{\mathrm{m}}}, \tag{9.31}$$

then the equation for the marginal state of monotonic instability in the absence of an imposed solutal gradient is

$$\mathrm{Ra} = \frac{4\pi^2}{1 + S(1 + \mathrm{Le})}. \tag{9.32}$$

The corresponding equation for marginal oscillatory instability is

$$\mathrm{Ra} = \frac{4\pi^2(\sigma + \varphi \mathrm{Le})}{\mathrm{Le}(\varphi + \sigma S)}. \tag{9.33}$$

The general situation, with both cross-diffusion and double diffusion (thermal and solutal gradients imposed), was analyzed by Patil and Rudraiah (1980). Taslim and Narusawa (1986) showed that there is an analogy between cross-diffusion (Soret and Dufour effects) and double diffusion in the sense that the equations can be put in mathematically identical form. A general study of the Soret effect in multicomponent flow was made by Lacabanne et al. (2002).

The linear analysis of Lawson et al. (1976), based on the kinetic theory of gases and leading to a Soret effect, was put forward to explain the lowering of the critical Rayleigh number in one gas due to the presence of another. This effect was observed in a binary mixture of helium and nitrogen by Lawson and Yang (1975). Lawson et al. (1976) observed that the critical Rayleigh number may be lower or greater than for a pure fluid layer depending upon whether thermal diffusion induces the heavier component of the mixture to move toward the cold or hot boundary, respectively. Brand and Steinberg (1983a) pointed out that with the Soret effect it is possible to have oscillatory convection induced by heating from above. Bedrikovetskii et al. (1993) included the effect of pressure work. Rudraiah

and Siddheshwar (1998) presented a weak nonlinear stability analysis with cross-diffusion taken into account. Ouarzazi et al. (2002) studied pattern formation in the presence of horizontal throughflow. Gaillard et al. (2003) investigated oscillatory convection in a geological environment. Costesèque et al. (2002) presented a synthesis of experimental and numerical studies.

The experimental and numerical study of Benano-Melly et al. (2001) was concerned with Soret coefficient measurement in a medium subjected to a horizontal thermal gradient. The onset of convection in a vertical layer subject to uniform heat fluxes along the vertical walls was treated analytically and numerically by Joly et al. (2001). The Soret effect also was included in the numerical study by Nejad et al. (2001). Sovran et al. (2001) studied analytically and numerically the onset of Soret-driven convection in an infinite horizontal layer with an applied vertical temperature gradient. They found that for a layer heated from above, the motionless solution is infinitely linearly stable in $N > 0$, while a stationary bifurcation occurs in $N < 0$. For a layer heated from below, the onset of convection is steady or oscillatory depending on whether N is above or below a certain value that depends on Le and the normalized porosity. The numerical study of Faruque et al. (2004) of the situation where fluid properties vary with temperature, composition, and pressure showed that for lateral heating the Soret effect was weak, but with bottom heating the Soret effect was more pronounced.

Further studies of Soret convection, building on studies discussed in Sect. 1.9, were reported by Jiang et al. (2004a, b, c) and by Saghir et al. (2005a). Attention has been placed on thermo-gravitational convection, a topic treated by Estebe and Schott (1970). This refers to a coupling effect when a fluid mixture saturating a vertical porous cavity in a gravitational field is exposed to a uniform horizontal thermal gradient, and thermo-diffusion produces a concentration gradient that leads to species separation. The porous media situation has been considered by Jamet et al. (1992) and Marcoux and Charrier-Mojtabi (1998). The numerical results of Marcoux and Mojtabi show the existence of a maximum separation corresponding to an optimal Rayleigh number as expected, but there remains a difference between the numerical results for that optimal value and experimental results of Jamet et al. (1992). The study by Jiang et al. (2004b) concentrated on the two-dimensional simulation of thermo-gravitation convection in a laterally heated vertical column with space-dependent thermal, molecular, and pressure diffusion coefficients taken as functions of temperature using the irreversible thermodynamics theory of Shukla and Firoozabadi. The numerical results reveal that the lighter fluid component migrates to the hot side of the cavity, and as the permeability increases the component separation in the thermal diffusion process first increases, reaches a peak, and then decreases. Jiang et al. (2004b) reported values of a separation ratio for a methane and n-butane mixture. Further studies of separation have been made by Er-Raki et al. (2008a, b) (vertical enclosure), Elhajjar et al. (2008, 2009, 2010) (horizontal or inclined cell), Bennacer et al. (2009) (multidomain separation), and Charrier-Mojtabi et al. (2011) (horizontal slot submitted to a heat flux) and Abahri et al. (2017) (horizontal annulus). Jiang et al. (2004c) explicitly investigated the effect of heterogeneous permeability, something that strongly affects the Soret

coefficient. Saghir et al. (2005a) have reviewed some aspects of thermo-diffusion in porous media.

Soret-driven convection in a shallow enclosure and with uniform heat (or both heat and mass) fluxes was studied analytically and numerically by Bourich et al. (2002, 2004e, f, 2005a, b), Er-Raki et al. (2005), and Bourich et al. (2016) (magnetic field). Depending on the values of Le and N, subcritical stationary convection may or may not be possible and parallel convective flow may or may not be possible. Convection in a shallow enclosure was also studied by Bourich et al. (2005a, b).

Enclosures heated and salted from the sides were studied by Er-Raki et al. (2006a, 2007, 2008, 2009, 2011). In this situation subcritical convection is possible.

An analytical and numerical study of convection in a horizontal layer with uniform heat flux applied at the horizontal walls, and with or without constant mass flux at those walls, was reported by Bahloul et al. (2003) and Boutana et al. (2004). A structural stability result was reported by Straughan and Hutter (1999).

Abbasi et al. (2011) studied the thermo-diffusion of carbon dioxide in various binary mixtures. Theoretical predictions of effective thermo-diffusion coefficients were made by Davarzani et al. (2010). A ternary mixture was examined by Jaber et al. (2008). Heterogeneous media were analyzed numerically by Jiang et al. (2006a). A doubly stratified medium was studied by Narayana and Murthy (2007). Nonlinear convection due to compositional and thermal buoyancy was treated by Tagare and Babu (2007). A strongly endothermic chemical reaction system was studied by Li et al. (2006a). Saravanan and Jegajoth (2010) examined a stationary fingering stability with coupled molecular diffusion and thermal nonequilibrium. Soret-driven convection in a cavity with perfectly conducting boundaries was analyzed by Lyubimov et al. (2011). Soret-driven convection in a horizontal layer in the presence of a heat or concentration source was studied by Goldobin and Lyubimov (2007). An analytical and numerical stability analysis of Soret-driven convection in a horizontal layer was made by Charrier-Mojtabi et al. (2007). A square cavity heated and salted from below was studied by Khadiri et al. (2010a). A square cavity with icy fluid was treated by Alloui et al. (2010a). The effect of anisotropy on linear and nonlinear convection in a horizontal layer was examined by Gaikwad et al. (2009a, b), while Gaikwad and Prasad (2011) studied the case of a couple-stress fluid. A study of stationary and oscillatory convection of binary fluids was made by Augustin et al. (2010).

Other studies involving cross-diffusion were made by Mansour et al. (2007a, b) (horizontal heat flux balanced by Soret mass flux), Motsa (2008), Rawat and Bhargava (2009) (micropolar fluid), Ahmed et al. (2011a, b) (vertical channel with magnetic field and chemical reaction), Jaimala and Goyal (viscoelastic fluid), Malashetty and Biradar (2012) (nonlinear stability), Gaikwad and Kamble (2012), Gaikwad and Kousar (2012) (rotation and chemical reaction), Patil and Parvathy (1989) (anisotropy), Malashetty and Biradar (2011b) (viscoelastic fluid), Gaikwad and Dhanraj (2014b) (viscoelastic fluid), Goyal and Jaimala (2012) (micropolar fluid), Gaikwad and Kamble (2014), (rotation, anisotropy), Saravanan and Keerthana (2012) (rotation), Rionero (2013a, b, c) (rotation), Ouattara et al.

(2012) (conducting boundary plates), Ferdows et al. (2013) (velocity and thermal slip, temperature-dependent viscosity, concentration-dependent diffusivity), Basu and Layek (2013) (heating and salting from above), Nik-Ghazali et al. (2014) (square annulus with cold inner surface and hot outer surface), Sekar et al. (2006) (ferrofluid), Li et al. (2013a) (endothermic reaction), Hidouri et al. (2013) (square cavity, entropy generation), Khidir and Sibanda (magnetic field, rotation), Sekar and Raju (2014) (ferrofluid, magnetic field dependent viscosity, anisotropy), Chamkha et al. (2014a) (rectangular duct, inclined magnetic field), Ajibade (2014) (vertical microchannel, dual-phase lag, unsteady flow), Altawallbeh et al. (2013a) (nonlinear stability, anisotropy, internal heat source), Wang et al. (2014a) (horizontal cavity), Roy and Murthy (2015) (horizontal channel, viscous dissipation), Augustin et al. (2015) (review), Yacine et al. (2016) (separation of binary mixtures, cross-heat fluxes), and Larabi et al. (2016) (ternary mixture).

The possible role of the Soret effect on the development of salinity gradients in geologic basins was discussed by Nield et al. (2013).

The topic of thermo-gravitational diffusion in a binary fluid was surveyed by Mojtabi et al. (2015).

9.1.5 Flow at High Rayleigh Number

The interaction between the heat transfer and mass transfer processes in the regime of strong convection was investigated on the basis of a two-dimensional model by Trevisan and Bejan (1987b). They used scale analysis to back up their numerical work. Figure 9.4 shows the main characteristics of the flow, temperature, and concentration fields in one of the rolls that form. This particular flow is heat transfer-driven in the sense that the dominant buoyancy effect is one due to temperature gradients ($N = 0$). The temperature field (Fig. 9.4b) shows the formation of thermal boundary layers in the top and bottom end-turn regions of the roll. The concentration field is illustrated in Fig. 9.4b–d. The top and bottom concentration boundary layers become noticeably thinner as Le increases from 1 to 20.

The overall Nusselt numbers Nu and overall Sherwood number Sh are defined by

$$\mathrm{Nu} = \frac{\bar{q}''}{k_\mathrm{m}\Delta T/H}, \quad \mathrm{Sh} = \frac{\bar{j}}{D_\mathrm{m}\Delta C/H} \tag{9.34}$$

where $\bar{q}''$ and $\bar{j}$ are the heat and mass fluxes averaged over one of the horizontal boundaries. In heat transfer-driven convection, $|N| << 1$, it is found that the Nusselt number scales as

$$\mathrm{Nu} = \left(\mathrm{Ra}/4\pi^2\right)^{1/2}. \tag{9.35}$$

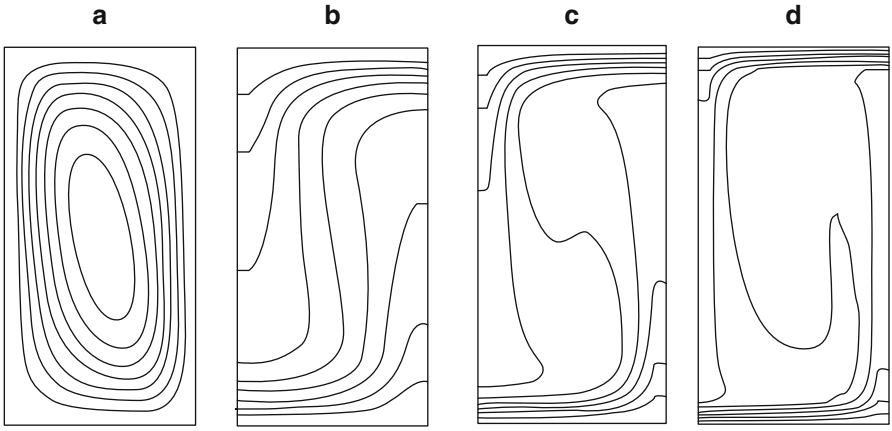

Fig. 9.4 Two-dimensional numerical simulation for heat transfer-driven ($N = 0$) convection in a horizontal porous layer (Ra = 200, $H/L = 1.89$). (**a**) Streamlines; (**b**) isotherms, also isosolutal lines for Le = 1; (**c**) isosolutal lines for Le = 4; and (**d**) isosolutal lines for Le = 20 (Trevisan and Bejan 1987b)

In the same regime the mass transfer scales are

$$\mathrm{Sh} \approx \mathrm{Le}^{1/2}\left(\mathrm{Ra}/4\pi^2\right)^{7/8} \text{ if } \quad \mathrm{Le} > \left(\mathrm{Ra}/4\pi^2\right)^{1/4}, \tag{9.36a}$$

$$\mathrm{Sh} \approx \mathrm{Le}^{2}\left(\mathrm{Ra}/4\pi^2\right)^{1/2} \text{ if } \quad \left(\mathrm{Ra}/4\pi^2\right)^{-1/4} < \mathrm{Le} < \left(\mathrm{Ra}/4\pi^2\right)^{1/4}, \tag{9.36b}$$

$$\mathrm{Sh} \approx 1 \text{ if } \quad \mathrm{Le} < \left(\mathrm{Ra}/4\pi^2\right)^{1/4}. \tag{9.36c}$$

The scales of mass transfer-driven flows, $|N| >> 1$, can be deduced from these by applying the transformation $\mathrm{Ra} \to \mathrm{Ra_D}$, $\mathrm{Nu} \to \mathrm{Sh}$, $\mathrm{Sh} \to \mathrm{Nu}$, and $\mathrm{Le} \to \mathrm{Le}^{-1}$. The results are

$$\mathrm{Sh} \approx \left(\mathrm{Ra_D}/4\pi^2\right)^{1/2}, \tag{9.37}$$

and

$$\mathrm{Nu} \approx \mathrm{Le}^{-1/2}\left(\mathrm{Ra_D}/4\pi^2\right)^{7/8} \text{if } \quad \mathrm{Le} < \left(\mathrm{Ra_D}/4\pi^2\right)^{-1/4}, \tag{9.38a}$$

$$\mathrm{Nu} \approx \mathrm{Le}^{-2}\left(\mathrm{Ra_D}/4\pi^2\right)^{1/2} \text{if } \quad \left(\mathrm{Ra_D}/4\pi^2\right)^{-1/4} < \mathrm{Le} < \left(\mathrm{Ra_D}/4\pi^2\right)^{1/4}, \tag{9.38b}$$

$$\mathrm{Nu} \approx 1 \text{ if } \quad \mathrm{Le} > \left(\mathrm{Ra_D}/4\pi^2\right)^{1/4}. \tag{9.38c}$$

These estimates agree well with the results of direct numerical calculations.

Rosenberg and Spera (1992) performed numerical simulations for the case of a fluid heated and salted from below in a square cavity. As the buoyancy ratio

N increases, the dynamics changes from a system that evolves to a well-mixed steady state, to one that is chaotic with large amplitude fluctuations in composition, and finally to one that evolves to a conductive steady state. Their correlations for Nu and Sh were in good agreement with the results of Trevisan and Bejan (1987b). Schoofs and Spera (2002) studied the transition to chaos.

Sheridan et al. (1992) found that their experimentally measured heat transfer data correlated well with $\mathrm{Nu} \sim (\mathrm{Ra}\,\mathrm{Da}\,N)^{0.294}\mathrm{Ja}^{-0.45}$. Here Ja is the Jakob number, defined by $\mathrm{Ja} = c_\mathrm{p}\Delta T/h_\mathrm{fg}\,\Delta\mathrm{m}$, where h_fg is the enthalpy of evaporation and m is the saturated mass ratio (vapor/gas).

9.1.6 Other Effects

9.1.6.1 Dispersion

If a net horizontal flow is present in the porous layer, it will influence not only the vertical solutal gradient but also the phenomenon of solute dispersion. Thermal dispersion also can be affected. In most applications α_m is greater than D_m, and as a consequence the solutal dispersion is more sensitive to the presence of through flow. The ultimate effect of dispersion is that the concentration distribution becomes homogeneous.

The stability implications of the anisotropic mass diffusion associated with an anisotropic dispersion tensor were examined by Rubin (1975b) and Rubin and Roth (1978, 1983). The dispersion anisotropy reduces the solutal stabilizing effect on the inception of monotonic convection and at the same time enhances the stability of the flow field with respect to oscillatory disturbances. Monotonic convection appears as transverse rolls with axes perpendicular to the direction of the horizontal net flow, while oscillatory motions are associated with longitudinal rolls (axes aligned with the net flow), the rolls of course being superposed on that net flow.

Certain geological structures contain some pores and fissures of large sizes. In such cavernous media even very slow volume-averaged flows can deviate locally from the Darcy flow model. The larger pores bring about an intensification of the dispersion of solute and heat and because of the high pore Reynolds numbers, Re_p, the effect of turbulence within the pores. Rubin (1976) investigated the departure from the Darcy flow model and its effect on the onset of convection in a horizontal layer with horizontal through flow. This study showed that in the case of laminar flow through the pores ($\mathrm{Re}_\mathrm{p} << 1$), the net horizontal flow destabilizes the flow field by enhancing the effect of solutal dispersion. A stabilizing effect is recorded in the intermediate regime ($\mathrm{Re}_\mathrm{p} \approx 1$). In the inertial flow regime ($\mathrm{Re}_\mathrm{p} >> 1$) the stability characteristics become similar to those of monodiffusive convection, the net horizontal flow exhibiting a stabilizing effect.

9.1.6.2 Anisotropy and Heterogeneity

The onset of thermohaline convection in a porous layer with varying hydraulic resistivity ($r = \mu/K$) was investigated by Rubin (1981). If one assumes that the dimensionless hydraulic resistivity $\xi = r/r_0$ varies only in the vertical direction and only by a relatively small amount, the linear stability analysis yields the monotonic marginal stability condition

$$\mathrm{Ra} + \mathrm{Ra_D} = \pi^2 \left(\xi_\mathrm{H}^{1/2} + \xi_\mathrm{V}^{1/2} \right)^2. \tag{9.39}$$

In this equation ξ_H and ξ_V are the horizontal and vertical mean resistivities

$$\xi_\mathrm{H} = \left(\int_0^1 \frac{d\hat{z}}{\xi} \right)^{-1}, \quad \xi_\mathrm{V} = \int_0^1 \xi d\hat{z}, \tag{9.40}$$

and so $\xi_\mathrm{H} \leq \xi_\mathrm{V}$. The right-hand side of Eq. (9.39) can be larger or smaller than $4\pi^2$ depending on whether Ra is based on ξ_V or ξ_H. A similar conclusion is reached with respect to the onset of oscillatory motions.

The Galerkin method has been used by Rubin (1982a) in an analysis of the effects of nonhomogeneous hydraulic resistivity and thermal diffusivity on stability. The effect of simultaneous vertical anisotropy in permeability (hydraulic resistivity), thermal diffusivity, and solutal diffusivity was investigated by Tyvand (1980) and Rubin (1982b).

Chen (1992) and Chen and Lu (1992b) analyzed the effect of anisotropy and inhomogeneity on salt-finger convection. They concluded that the critical Rayleigh number for this is invariably higher than that corresponding to the formation of plumes in the mushy zone during the directional solidification of a binary solution (see Sect. 10.2.3). A numerical study of double-diffusive convection in layered anisotropic porous media was made by Nguyen et al. (1994).

Viscosity variations and their effects on the onset of convection were considered by Patil and Vaidyanathan (1982), who performed a nonlinear stability analysis using the Brinkman equation, assuming a cosine variation for the viscosity. The variation reduces the critical Rayleigh number based on the mean viscosity. Bennacer (2004) treated analytically and numerically a two-layer (one anisotropic) situation with vertical through mass flux and horizontal through heat flux. Nield and Kuznetsov (2013e) investigated a two-layer system with internal heating. Nield et al. (2015) studied the effect of local thermal nonequilibrium in a two-layer system.

Heterogeneity effects were also studied by Alloui et al. (2009a), Jaber and Saghir (2011), Kuznetsov and Nield (2008b), Sammouda et al. (2013) (nonuniform porosity), and Elbouzidi et al. (2014a, b). The case of depth-dependent viscosity and permeability was studied by Rionero (2014b).

Anisotropy was also treated by Malashetty (1993), Malashetty and Gaikwad (2002), Malashetty and Swamy (2010b), Malashetty and Biradar (2011a), while

Subramanian and Patil (1991) combined anisotropy with cross-diffusion. Harfash (2016d) combined heterogeneity and anisotropy.

9.1.6.3 Brinkman Model

The effect of porous medium coarseness on the onset of convection was documented by Poulikakos (1986). With the Brinkman equation the critical Rayleigh number for the onset of monotonic instability is given by

$$\mathrm{Ra} + \mathrm{Ra_D} = \frac{\left(\alpha_c^2 + \pi^2\right)^2}{\alpha_c^2}\left[\left(\alpha_c^2 + \pi^2\right)\widetilde{\mathrm{Da}} + 1\right], \tag{9.41}$$

where the critical dimensionless horizontal wavenumber (α_c) is given by

$$\alpha_c^2 = \frac{\left(\pi^2\widetilde{\mathrm{Da}} + 1\right)^{1/2}\left(9\pi^2\widetilde{\mathrm{Da}} + 1\right)^{1/2} - \pi^2\widetilde{\mathrm{Da}} - 1}{4\widetilde{\mathrm{Da}}}. \tag{9.42}$$

In terms of the effective viscosity $\widetilde{\mu}$ introduced in Eq. (1.17), the Darcy number $\widetilde{\mathrm{Da}}$ is defined by

$$\widetilde{\mathrm{Da}} = \frac{\widetilde{\mu}}{\mu}\frac{K}{H^2}. \tag{9.43}$$

Nonlinear energy stability theory was applied to this problem by Guo and Kaloni (1995b). Fingering convection, with the Forchheimer term as well as the Brinkman term taken into account, was treated numerically by Chen and Chen (1993a, b). With Ra fixed, they found a transition from steady to time-periodic (and then to quasiperiodic) convection as $\mathrm{Ra_D}$ increases. An analytical solution based on a parallel flow approximation and supported by numerical calculations was presented by Amahmid et al. (1999a). They showed that there is a region in the (N, Le) plane where a convective flow of this type is not possible for any Ra and Da values. A linear and nonlinear stability analysis leading to calculations of Nusselt numbers, streamlines, isotherms, and isohalines was presented by Shivakumara and Sumithra (1999). The Brinkman model was also used by Wang and Tan (2009). Further work with the Brinkman model and a horizontal cavity was done by Alloui et al. (2010b).

The ultimate boundedness and stability of triply diffusive mixtures in rotating layers was studied by Capone and de Luca (2012b). Kaloni and Guo (1996) obtained a weak nonlinear solution and investigate the existence, regularity, and uniqueness of a solution. The structural stability for Brinkman convection, with a chemical reaction in which the solubility depends on temperature, was investigated by Straughan and Al Sulaimi (2014).

9.1.6.4 Additional Effects

Multicomponent Convection

Triple diffusion was treated by Rudraiah and Vortmeyer (1982), Poulikakos (1985c), and Tracey (1996), who obtained some unusual neutral stability curves, including a closed approximately heart-shaped oscillatory curve disconnected from the stationary neutral curve, and thus requiring three critical values of Ra to describe the linear stability criteria. For certain values of parameters the minima on the oscillatory and stationary curves occur at the same Rayleigh number but different wavenumbers. Tracey (1998) studied the case of penetrative convection. Further studies were made by Chand (2012) (magnetized ferrofluid with internal angular momentum), Bulgarkova (2012) (rectangular box, modulation of the concentration gradient), Chand (Chand 2013a, Chand 2013b) (micropolar ferromagnetic fluid), Capone and De Luca (2012a), Wang et al. (2014a, b) (Maxwell viscoelastic fluid, heated from below or internally), and Rionero (2011c, 2012a, b, 2013c, 2014a, b, 2015) (global nonlinear stability, depth-dependent viscosity, and permeability). A multicomponent fluid was investigated numerically by Kantur and Tsibulin (2004). Multiple diffusion results for ultimate boundedness, absence of subcritical instability, and global nonlinearity were obtained by Rionero (2013a, b, c). Rionero (2014a) studied a multicomponent fluid in a rotating horizontal layer heated from below and salted partly from below and partly from above, with emphasis on the conditions for the instability of the thermal conduction solution irrespective of the temperature gradient. Prakash et al. (2016c) discussed the limitations of linear growth rates in triply diffusive convection. Prakash et al. (2016d) treted convection in a cylindrical slab for the case of large viscosity variation.

Magnetic Field

A ferromagnetic fluid was treated by Vaidyanathan et al. (1995), Sekar et al. (1998) (rotation), Sunil et al. (2004b, 2005a, b, c, 2007, 2009a, 2010b), Divya et al. (2005), Sunil and Sharma (2005a, b, c, d, e, f, g), Sunil and Mahajan (2008a, 2009a, b), and Sekar and Raju (2015) (micropolar fluid). These papers covered both linear and nonlinear stability and the various effects of rotation, micropolar fluid, magnetic-field-dependent viscosity, suspended dust particles, and local thermal nonequilibrium.

When the fluid is not a ferrofluid, the effect of a magnetic field is usually unimportant for a regular porous medium (an exception is a mushy zone) because it is not possible to produce a magnetic field strong enough for the magnetic drag to be significant in comparison with the Darcy drag. We briefly mention the papers by Sharma and Sharma (1980), Sharma and Kumari (1992) (rotation), Sharma and Bhardwaj (1993) (rotation), Sunil (1994, 1999, 2001) (compressibility), Prakash

and Manchanda (1994) (partly ionized plasma), Khare and Sahai (1993) (heterogeneity), Chamkha and Al-Naser (2002) (binary gas), Ramanbason and Vasseur (2007), Shihari and Rao (2008), Bourich et al. (2008) (external shear stress), Srivastava et al. (2012) (anisotropy, Soret effect), Salem and Fathy (2012), Altawallbeh et al. (2013b, d) (heating from below, cooling from the side), Haque et al. (2013) (rotation, unsteady flow), Benerji Babu et al. (2014) (nonlinear stability), Harfash and Alshara (2015a, b) (throughflow, anisotropy, internal heating, and then chemical reaction, variable gravity), Harfash and Alshara (2015b) (throughflow, internal heating, anisotropy), Kumar et al. (2015e) (triple diffusion, viscoelastic fluid), and Bourich et al. (2016) (Soret effect, uniform fluxes of heat and mass). Shekar et al. (2016) (inclined square, cross-diffusion) and Prakash and Gupta (2016) (conditions for the nonexistence of oscillatory motions) and Zhao et al. (2016) (fractional Maxwell fluid).

Papers on MHD convection with a non-Newtonian fluid are those by Sharma and Sharma (1990, 2000), Sharma and Kumar (1996), Sharma and Thakur (2000), Sharma and Kishor (2001), Sharma et al. (2001), Sunil et al. (2001), Kumar and Mohan (2011, 2012c), Kumar (2012b), Kumar et al. (2013c) (rotation), Rana (2013, 2014) (viscoelastic fluid, suspension, variable gravity, rotation), Kumar et al. (2013c) (viscoelastic fluid, rotation), Kumar (2016) (micropolar fluid, radiation, chemical reaction).

Rotation

The effect of rotation was included by Chakrabarti and Gupta (1981), Raptis (1983a), Rudraiah et al. (1986), (anisotropic media), Patil et al. (1989, 1990) (anisotropy), Malashetty and Begum (2011a) (anisotropy), Saravanan and Keerthana (2012), Falsaperla et al. (2012) (general boundary conditions), Gaikwad and Begum (2013) (reaction-convection, anisotropy), Bhadauria et al. (2013c) (cross-diffusion, anisotropy), Rionero (2014d) (nonlinear stability), Capone and De Luca (2014b) (vertical throughflow), Alhusseny and Turan (2015a, b) (long rotating channel), and Gaikwad and Kamble (2016) (couple-stress fluid, cross-diffusion, anisotropy).

Non-Newtonian Fluid

Papers involving a rotating non-Newtonian fluid are those by Sharma et al. (1998, 1999a) and Sharma and Rana (2001, 2002), Reena and Rana (2009), Kumar and Bhadauria (2011c), Malashetty and Swamy (2010b, 2011a), b, Bhadauria (2011), Malashetty et al. (2013), Rana and Thakur (2013a) (suspension), Rana and Thakur (2013b) (couple-stress fluid), and Rana et al. (2012c) (compressible Walters model B′ fluid).

Non-Newtonian fluids permeated with suspended particles have been studied by Sharma et al. (1999b), Sunil et al. (2003b, 2004d), Sharma and Sharma (2004), and

Rana et al. (2012c). Other papers on non-Newtonian fluids of various sorts are those by Sharma and Kumari (1993), Awad et al. (2010) (Maxwell fluid), Malashetty et al. (2009c, e, 2010b, 2011), (viscoelastic fluid, anisotropy), Kumar and Bhadauria (2011b) (viscoelastic fluid, thermal nonequilibrium), Malashetty and Swamy (2011a, b) (viscoelastic fluid, rotation, anisotropy), Malashetty and Kollur (2011) (couple-stress fluid, anisotropy), Malashetty et al. (2010a) (couple-stress fluid), Wang and Tan (2008c, 2011) (Maxwell fluid, cross-diffusion), Shivakumara et al. (2011j, 2013b) (couple-stress fluid), Narayana et al. (2012a) (Maxwell fluid), Swamy et al. (2012) (viscoelastic fluid), Swamy et al. (2012), Ben Khelifa et al. (2012), Delenda et al. (2012) (viscoelastic fluid), Chand and Rana (2012b) (cross-diffusion, viscoelastic fluid), Gaikwad and Birada (2013), Gaikwad and Kouser (2013), Srivastava and Bera (2013) (couple-stress fluid, chemical reaction), Liu and Umavathi (2013) (micropolar fluid), Gaikwad and Kouser (2013, 2014) (internal heating, viscoelastic and couple-stress fluid), Zhao et al. (2014b) (internal heat source, nonlinear stability), Gaikwad and Dhanraj (2014b) (anisotropy, internal heat source), and Zhu et al. (2017a) (power-law fluid, anisotropy, unsteady flow, 3D numerical investigation), Zhu et al. (2017b) (power law fluid, entropy production, heterogeneity), Zheng et al (2016) (Marangoni effect, volumetric heat generation, chemical reaction) and Thirumurugan and Vasanthakumari (2016) (Walters visco-elastic fluid, suspension. A viscoelastic fluid with local thermal nonequilibrium was examined by Malashetty et al. (2012a) and Yang et al. (2013).

Local Thermal Nonequilibrium

The effect of thermal nonequilibrium was added by Malashetty et al. (2008, 2009a), Malashetty and Heera (2008a, b, 2009), and Chen et al. (2011).

Throughflow

The effect of vertical throughflow was studied by Shivakumara and Khalili (2001), Shivakumara and Nanjundappa (2006) (quadratic drag), Shivakumara and Sureshkumar (quadratic drag, Oldroyd-B fluid), Pieters and Schuttlelaars (2008) (nonlinear dynamics), Capone et al. (2013, 2014), Capone and De Luca (2014a, b) (nonlinear stability, variable diffusivities), Harfash and Hill (2014) (internal heating, anisotropy, 3D simulation), Kiran (2015b, 2016c) (nonuniform effects, g-jitter effects), and Deepika and Narayana (2016) (nonlinear stability, concentration-based internal heat source). The effect of horizontal through flow was investigated by Joulin and Ouarzazi (2000), Lyubimov et al. (2008a), Matta et al. (2016a, b) (variable gravity, internal heat source, nonlinear stability), and Deepika et al. (2016) (concentration-based internal heat source).

Thermal Modulation

The effect of temporally fluctuating temperature on instability was analyzed by Ouarzazi and Bois (1994), Ouarzazi et al. (1994), McKay (1998b, 2000), Ramazanov (2001), and Malashetty and Basavaraja (2004). The last study included the effect of anisotropy. The studies by McKay make use of Floquet theory. He demonstrated that the resulting instability may be synchronous, subharmonic, or at a frequency unrelated to the heating frequency.

The effect of modulated temperature at the boundaries was considered by Ramazanov (2001), Bhadauria (2007b, c), Bhadauria and Sherani (2008b), and Bhadauria and Srivastava (2010) (MHD). Chaotic behavior induced by thermal modulation was studied by Malasoma et al. (1999). Resonance induced by sinusoidal heat was investigated by El Ayachi et al. (2010). Periodic heating of a square enclosure with crossed temperature and concentration gradients was examined by Abourida et al. (2011).

Vibration

The effect of vertical vibration was studied analytically and numerically by Sovran et al. (2000, 2002) and Jounet and Bardan (2001). Depending on the governing parameters, vibrations are found to delay or advance the onset of convection, and the resulting convection can be stationary or oscillatory. An intensification of the heat and mass transfers is observed at low frequency for sufficiently high vibration frequency. The onset of Soret-driven convection with a vertical variation of gravity was analyzed by Alex and Patil (2001) and Charrier-Mojtabi et al. (2004, 2005). The latter considered also horizontal vibration and reported that for both monotonic and oscillatory convection the vertical vibration has a stabilizing effect while the horizontal vibration has a destabilizing effect on the onset of convection. A further study of the effect of vibration was made by Strong (2008a, 2009). The effect of vibration on a system with a horizontal layer of clear fluid overlying a horizontal porous layer was studied by Lyubimov et al. (2008b).

The effect of g-jitter with a viscoelastic fluid and local thermal nonequilibrium was studied by Suthar et al. (2012). The effect of g-jitter with a composite fluid/porous layer was investigated by Swamy (2014a). The combination of thermal and gravity modulation was treated by Siddheswar et al. (2012b).

Groundwater Studies

The problem of convection in groundwater below an evaporating salt lake was studied in detail by Wooding et al. (1997a, b) and Wooding (2007). Now the convection is driven by the evaporative concentration of salts at the land surface, leading to an unstable distribution of density, but the evaporative groundwater discharge dynamically can stabilize this saline boundary layer. The authors

investigated the nature, onset, and development (as fingers or plumes) of the convection. They reported the result of linear stability analysis, numerical simulation, and laboratory experimentation using a Hele-Shaw cell. The results indicate that in typical environments, convection will predominate in sediments whose permeability exceeds about 10^{-14} m^2, while below this threshold the boundary layer should be stabilized, resulting in the accumulation of salts at the land surface. A numerical model simulating this situation was presented by Simmons et al. (1999). A related problem involving the evaporation of groundwater was studied analytically and numerically by Gilman and Bear (1996). The groundwater flow pattern in the vicinity of a salt lake also has been studied numerically by Holzbecher (2005b). A numerical study of convection above a salt dome was made by Holzbecher et al. (2010). A stability aspect of hot springs was studied by Bera et al. (2011). The onset of convection in groundwater wells was examined by Love et al. (2007). The onset of convection in under-ice melt ponds was investigated by Hirata et al. (2012).

Chemical Reaction

The situation in which one of the components undergoes a slow chemical reaction was analyzed by Patil (1982a), while a convective instability that is driven by a fast chemical reaction was studied by Steinberg and Brand (1983, 1984). Further work involving chemical reactions was carried out by Subramanian (1994), Malashetty et al. (1994), and Malashetty and Gaikwad (2003).

The effects of chemical reaction with double dispersion were examined by El-Amin et al. (2008). Li et al. (2006a, b, c, 2007, 2013a, b) examined various combinations of cross-diffusion, endothermic reactions, local thermal nonequilibrium, and forced convection. The onset of convection driven by a catalytic surface reaction was studied by Postelnicu (2009) and Scott and Straughan (2011); in the latter paper it was shown that if the reaction parameter exceeds a certain value then convection appears as oscillatory (rather than stationary) convection. Prichard and Richardson (2007) studied the effect of temperature-dependent solubility. The case of strong exothermic chemical reaction with local thermal nonequilibrium was studied by Bousri et al. (2012). Scott (2012a, b) studied the case of a layer with an exothermal surface reaction at the lower boundary, with and without the Soret effect. The effect of a reaction at the surface of a porous medium was also studied by Scott (2013a, b) and Scott and Straughan (2013b). Kim and Choi (2014b) studied the effect of first-order chemical reaction on gravitational instability. Al-Sulaimi (2015) presented an energy stability analysis. A case where the dissolved reaction component concentration is a function of temperature was studied by Straughan (2015b). A nonlinear stability analysis for a problem with chemical reaction was presented by Al-Sulaimi (2016) and Gaikwad and Dhanraj (2016) (anisotropy).

Internal Heating

The critical conditions for the onset of convection in a doubly diffusive porous layer with internal heat generation were documented by Selimos and Poulikakos (1985). The effect of heat generation or absorption was also studied by Chamkha (2002). Heat generation with anisotropy was studied by Bhadauria (2012) and Gaikwad and Dhanraj (2015). A case with local nonuniform thermal equilibrium was dealt with by Zhang et al. (2015a, b, c). The effects of local thermal equilibrium and vertical heterogeneity were analyzed by Kuznetsov et al. (2015).

Composite Domains

Fluid-porous composite media were studied by Gobin and Goyeau (2010), Hill and Carr (2013a, b) (stability of solar ponds), Jena et al. (2013c), and Olali (2013) (selective absorption of radiation).

Other Studies

Convective stability of a binary mixture in a fractured porous medium was studied by Bedrikovetskii et al. (1994). An experimental study involving an electrochemical effect when horizontal temperature and concentration gradients are imposed was reported by Chen (1998d). A transport correlation was presented by Yoon et al. (2001). Flow transitions in three-dimensional fingering were studied by Sezai (2002). Younsi et al. (2002a, b) studied a 2D box with horizontal gradients and opposing flow. Carr (2003b) modeled the evolution of under-ice melt ponds.

Kalla et al. (2001a) studied a situation involving imposed vertical heat and mass fluxes and a horizontal heat flux that they treated as a perturbation leading to asymmetry of the bifurcation diagram. Multiple steady-state solutions, with different heat and mass transfer rates, were found to coexist. Two and three-dimensional multiple steady states were studied by Khadiri et al. (2011). Multiple steady states in an enclosure partly heated and fully salted from below were examined by Alloui et al. (2009b). In their analytical studies Masuda et al. (1999, 2002) found that there is a range of buoyancy ratios N for which there is an oscillation between two types of solution, temperature dominated and concentration dominated. Some mathematical aspects were studied by Franchi and Straughan (1993), Lin and Payne (2007), Rionero (2007, 2010, 2012c), and Rionero and Vergori (2010). The boundary domain integral method was used by Kramer et al. (2007) and Jeci et al. (2009). Convection in an enclosure with partial or localized heating and salting was studied by Zhao et al. (2008b, c). Turbulent convection was treated by Tofaneli and de Lemos (2009). Lin (1992) studied numerically a transient problem. For the case of a cavity heated and salted from below, Khadiri et al. (2010b) made a comparison of two-dimensional and three-dimensional models. The effect of viscous dissipation was examined by Barletta and Nield (2011b). Tipping points for convection with a

Cattaneo–Christov fluid were studied by Straughan (2011b). Umla et al. (2011) studied three-dimensional pattern formation. Kim and Choi (2012) studied the effect of an impulsive change in concentration at the upper boundary. Convection due to a wavy horizontal surface was investigated by Narayana and Sibanda (2012). Kuznetsov and Nield (2012c) studied the onset of double-diffusive convection in a vertical cylinder occupied by a heterogeneous porous medium with vertical throughflow. Convection in a cavity for the case of a density maximum was treated by Muthtamilselvan and Das (2012). Benerji Babu et al. (2012b) studied linear and weakly nonlinear stability in the presence of radiation. Musuuza et al. (2012) studied a box with a partly heated bottom. Bahadori and Rezvantalab (2014) investigated the effects of viscosity dependent on temperature and concentration. Altawallbeh et al. (2013c) examined a cavity partly heated from below and partly heated from the side. Lo Jacono et al. (2013) studied three-dimensional spatially localized binary convection. Straughan (2014a) investigated an anisotropic inertia effect in microfluidic convection. Jamshidzadeh et al. (2013) studied the thermohaline extension of the Henry and Elder problems (unevenly heated bottom wall) with dispersion effects. The effect of variable gravity on linear and nonlinear stability of Hadley flow was investigated by Matta and Lakshmi Narayana (2016).

9.2 Horizontal Heat and Mass Transfer

9.2.1 Boundary Layer Flow and External Natural Convection

The most basic geometry for simultaneous heat and mass transfer from the side is the vertical wall embedded in a saturated porous medium. Specified at the wall are the uniform temperature T_0 and the uniform concentration C_0. The temperature and concentration sufficiently far from the wall are T_∞ and C_∞.

The Darcy flow driven by buoyancy in the vicinity of the vertical surface can have one of the four two-layer structures shown in Fig. 9.5. The thicknesses δ, δ_T, and δ_C indicate the velocity, thermal, and concentration boundary layers. The relative size of these three thicknesses is determined by the combination (N, Le).

The heat and mass transfer from the vertical surface was determined first based on scale analysis (Bejan 1984, pp. 335–338) and later based on the boundary layer similarity method (Bejan and Khair 1985). The results of the scale analysis are summarized in Table 9.1. Each row in this table corresponds to one of the quadrants of the (N, Le) domain covered by Fig. 9.5. The v scale represents the largest vertical velocity, which in Darcy flow occurs right at the wall. By writing this time $\bar{q}''$ and $\bar{j}$ for the heat and mass fluxes averaged over the wall height H, the overall Nusselt and Sherwood numbers are defined as

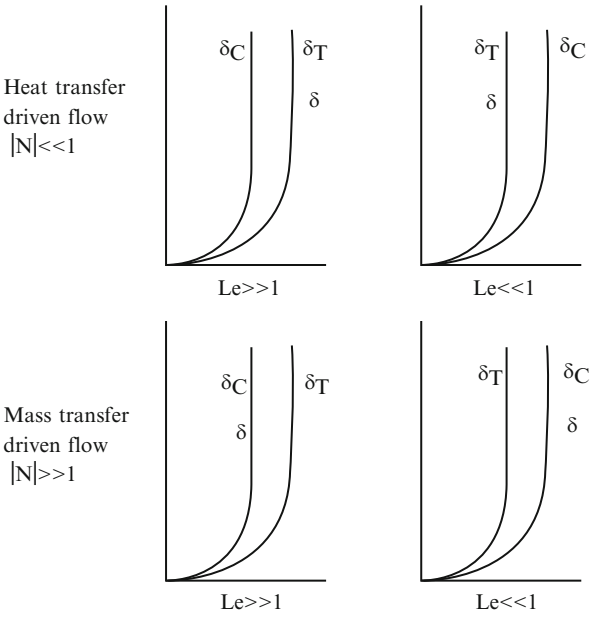

Fig. 9.5 The four regimes of boundary layer heat and mass transfer near a vertical surface embedded in a porous medium (Bejan and Khair 1985)

Table 9.1 The flow, heat, and mass transfer scales for the boundary layer near a vertical wall embedded in a porous medium (Bejan 1984, Bejan and Khair 1985)

Driving mechanism	v	Nu	Sh	Le domain
Heat transfer	(α_m/H) Ra	$\mathrm{Ra}^{1/2}$	$(\mathrm{Ra\ Le})^{1/2}$	Le >> 1
($\|N\|$ << 1)	(α_m/H) Ra	$\mathrm{Ra}^{1/2}$	$\mathrm{Ra}^{1/2}$ Le	Le << 1
Mass transfer	(α_m/H) Ra$\|N\|$	$(\mathrm{Ra}\|N\|)^{1/2}$	$(\mathrm{Ra}\|N\|\mathrm{Le})^{1/2}$	Le << 1
($\|N\|$ >> 1)	(α_m/H) Ra$\|N\|$	$\mathrm{Le}^{-1/2}(\mathrm{Ra}\|N\|)^{1/2}$	$(\mathrm{Ra}\|N\|\mathrm{Le})^{1/2}$	Le >> 1

$$\mathrm{Nu} = \frac{\bar{q}''}{k_m(T_0 - T_\infty)/H}, \quad \mathrm{Sh} = \frac{\bar{j}}{D_m(C_0 - C_\infty)/H}. \tag{9.44}$$

The similarity solution to the same problem was obtained by Bejan and Khair (1985) by selecting the nondimensional similarity profiles recommended by the scale analysis (Table 9.1).

$$u = -\frac{\alpha_m}{x}\mathrm{Ra}_x f'(\eta), \tag{9.45}$$

$$v = -\frac{\alpha_m}{2x}\mathrm{Ra}_x^{1/2}(f - \eta f'), \tag{9.46}$$

$$\theta(\eta) = \frac{T - T_\infty}{T_0 - T_\infty}, \quad \eta = \frac{y}{x}\mathrm{Ra}_x^{1/2}, \tag{9.47}$$

$$c(\eta) = \frac{C - C_\infty}{C_0 - C_\infty}. \tag{9.48}$$

In this formulation, x is the distance measured along the wall and the Rayleigh number is defined by $\mathrm{Ra}_x = g\beta\, Kx(T_0 - T_\infty)/\nu\alpha_\mathrm{m}$. The equations for momentum, energy, and chemical species conservation reduce to

$$f'' = -\theta' - Nc', \tag{9.49}$$

$$\theta'' = \frac{1}{2} f\theta', \tag{9.50}$$

$$c'' = \frac{1}{2} fc'\mathrm{Le}, \tag{9.51}$$

with the boundary conditions $f = 0$, $\theta = 1$, and $c = 1$ at $\eta = 0$, and $(f, \theta, c) \to 0$ as $\eta \to \infty$. Equations (9.49)–(9.51) reinforce the conclusion that the boundary layer phenomenon depends on two parameters, N and Le.

Figure 9.6 shows a sample of vertical velocity and temperature (or concentration) profiles for the case $\mathrm{Le} = 1$. The vertical velocity increases and the thermal boundary layer becomes thinner as $|N|$ increases. The same similarity solutions show that the concentration boundary layer in heat transfer-driven flows ($N = 0$) becomes thinner as Le increases, in good agreement with the trend anticipated by scale analysis.

The effect of wall inclination on the two-layer structure was described by Jang and Chang (1988b, c). Their study is a generalization of the similarity solution

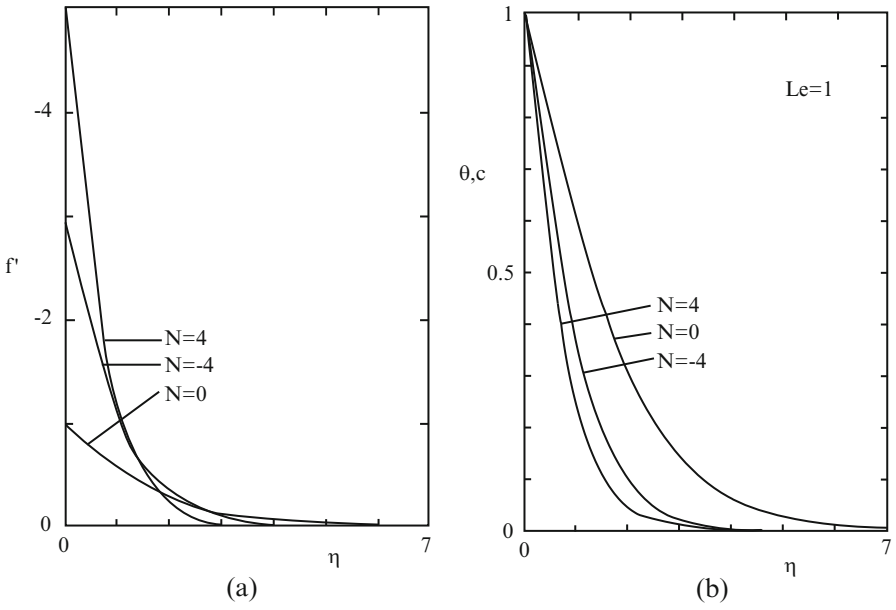

Fig. 9.6 The buoyancy ratio effect on the $\mathrm{Le} = 1$ similarity profiles for boundary layer heat and mass transfer near a vertical wall embedded in a porous medium. (**a**) Velocity profiles and (**b**) temperature and concentration profiles (Bejan and Khair 1985)

Table 9.2 The flow, heat, and mass transfer scales for the boundary layer near a horizontal wall embedded in a saturated porous medium (Jang and Chang 1988b)

Driving mechanism	u	Nu	Sh	Le domain
Heat transfer	$(\alpha_m/H)\mathrm{Ra}^{2/3}$	$\mathrm{Ra}^{1/3}$	$\mathrm{Ra}^{1/3}\mathrm{Le}^{1/2}$	$\mathrm{Le} >> 1$
($\lvert N\rvert << 1$)	$(\alpha_m/H)\mathrm{Ra}^{2/3}$	$\mathrm{Ra}^{1/3}$	$\mathrm{Ra}^{1/3}\mathrm{Le}$	$\mathrm{Le} << 1$
Mass transfer	$(\alpha_m/H) \times (\mathrm{Ra}\lvert N\rvert)^{2/3}\mathrm{Le}^{-1/3}$	$(\mathrm{Ra}\lvert N\rvert)^{-1/3}\mathrm{Le}^{-1/6}$	$(\mathrm{Ra}\lvert N\rvert\mathrm{Le})^{1/3}$	$\mathrm{Le} << 1$
($\lvert N\rvert >> 1$)	$(\alpha_m/H) \times (\mathrm{Ra}\lvert N\rvert)^{2/3}\mathrm{Le}^{-1/3}$	$(\mathrm{Ra}\lvert N\rvert)^{-1/3}\mathrm{Le}^{-2/3}$	$(\mathrm{Ra}\lvert N\rvert\mathrm{Le})^{1/3}$	$\mathrm{Le} >> 1$

approach employed by Bejan and Khair (1985). The heat and mass transfer scales that prevail in the extreme case when the embedded H-long surface is horizontal are summarized in Table 9.2. A related study was reported by Jang and Ni (1989), who considered the transient development of velocity, temperature, and concentration boundary layers near a vertical surface. Further studies were made by Bestman (1989).

The effect of flow injection on the heat and mass transfer from a vertical plate was investigated by Lai and Kulacki (1991d): see also the comments by Bejan (1992a). Raptis et al. (1981a, b) showed that an analytical solution is possible in the case of an infinite vertical wall with uniform suction at the wall-porous medium interface. The resulting analytical solution describes flow, temperature, and concentration fields that are independent of the vertical coordinate. This approach was extended to the unsteady boundary layer flow problem by Raptis and Tzivanidis (1984). Raptis et al. (1981a, b) and Raptis (1983c) studied the case of constant suction with time-dependent temperature. Das et al. (2006) studied constant suction and a source/sink. For the case of a non-Newtonian (power-law) fluid, an analytical and numerical treatment was given by Rastogi and Poulikakos (1995). The case of a thermally stratified medium was studied numerically by Angirasa et al. (1997). Nonsimilar solutions for the case of two prescribed thermal and solutal boundary conditions were obtained by Aly and Chamkha (2010).

The physical model treated by Bejan and Khair (1985) was extended to the case of a boundary of arbitrary shape by Nakayama and Hossain (1995). A further scale analysis of natural convection boundary layers driven by thermal and mass diffusion was made by Allain et al. (1992), who also made some corroborating numerical investigations. They noted the existence of flows that are heat driven even though the amplitude of the solutal convection is dominant. Bansod and Jadhav (2010) obtained an analytical solution of the Bejan-Khair equation. Aouachria (2009), using an integral method, obtained results agreeing with those of Bejan and Khair (1985).

An analytical-numerical study of hydrodynamic dispersion in natural convection heat and mass transfer near vertical surfaces was reported by Telles and Trevisan (1993). They considered flows due to a combination of temperature and concentration gradients and found that four classes of flows are possible according to the relative magnitude of the dispersion coefficients.

For convection over a vertical plate, the Forchheimer effect was analyzed by Murthy and Singh (1999); dispersion effects were studied by Khaled and Chamkha (2001), Chamkha and Quadri (2003), and El-Amin (2004a), and the effect of double stratification was discussed by Bansod et al. (2002) and Murthy et al. (2004b). Chamkha (2001a) treated a nonisothermal permeable plate. Using homotopy analysis and the Forchheimer model, an analytic solution was obtained by Wang et al. (2003a). The effect of thermophoresis particle deposition was analyzed by Chamkha and Pop (2004), Ganesan et al. (2014) (stratification), and Kameswaran et al. (2014b). Three-dimensional flow was treated by Singh (2005), Chamkha et al. (2006a), and Duwairi and Damseh (2008b, 2009) (radiation, mixed convection). The case of density depending on temperature and concentration in a nonlinear manner was studied by Partha (2010) and Bég et al. (2009c) (time dependence, radiation). Other studies were made by Singh and Queeny (1997), Singh (2007), Singh et al. (2007) (periodic permeability, variable suction), Ferdows et al. (2008) (cross-diffusion), El-Arabawy (2009) (cross-diffusion, variable wall temperature), (variable conductivity, slip), Moorthy and Senthilvadivu (2012a), c) (variable viscosity, cross-diffusion), Srinivasacharya et al. (2015c, d) (double stratification, spectral quasilinearization), Srinivasacharya and Surenda (2016) (cross-diffusion, double stratification), Huang (2016a, b) (cross-diffusion, radiation, internal heating), and Loganathan and Sivapoornapriya (2016b) (impulsively started plate, chemical reaction).

9.2.1.1 Magnetic Field

Except when the fluid is ferrofluid or the medium is a mushy zone, the effect of convection in a regular fluid is generally insignificant. It is not possible to produce a magnetic field strong enough for the magnetic drag to become significant in comparison with the Darcy drag. Nevertheless a large number of theoretical papers involving a magnetic field have been published.

MHD convection was treated for a vertical plate by Singh et al. (1991) (rotation, unsteady flow), Cheng (1999, 2005), Chamkha and Khaled (2000c, d), Acharya et al. (2000), Hassanien and Allah (2002) (pulsating permeability), Takhar et al. (2003a, b) (unsteady flow), Kim (2004) (micropolar fluid, moving plate), Postelnicu (2006), Chaudhary and Jain (2007a) (oscillating plate), Chaudhary and Jain (2007b) (micropolar fluid, radiation, variable permeability, slip flow), Afifi (2007a) (cross-diffusion, temperature-dependent viscosity), Ahmed (2007) (unsteady flow), Prasad and Reddy (2008) (transient), Eldabe et al. (2008) (Eyring-Powell fluid), Das et al. (2009a, b) (oscillatory suction), Al-Odat et al. (2009) (transient), Sudheer Babu and Satya Narayana (2009) (chemical reaction, radiation absorption, variable suction), Singh and Kumar (2010) (transient), Sharma et al. (2010) (transient), Jang and Hsu (2009a) (Hall effect), Kamel (2001) (unsteady flow), Makinde (2009a, 2011a, 2012) (radiation, chemical reaction, stagnation point flow), Makinde and Sibanda (2008), Postelnicu (2004) (double diffusion), Jain et al. (2009) (radiation, slip), Ferdows and Chen (2009) (cross-diffusion), Kishan et al. (2009) (double

stratification, viscous dissipation), Dash et al. (2009a, b) (viscoelastic fluid, rotation, chemical reaction), Kairi et al. (2009) (double dispersion), Dash et al. (2011) (Oldroyd fluid, rotation), Ramana Reddy et al. (2010), Tak et al. (2010a, b) (cross-diffusion, radiation), Hayat et al. (2010c) (unsteady flow), Ramachandra Prasad et al. (2011) (cross-diffusion), Rashad et al. (2011a) (chemical reaction, stretching sheet), Osman et al. (2011a, b), Kesavaiah et al. (2011a, b) (chemical reaction, radiation absorption, unsteady flow, moving plate with suction, heat source), Al-Odat and Al-Ghamdi (2012) (cross-diffusion, unsteady flow), Sahoo and Dash (2012), Salem and Fathy (2012) (stagnation point flow, stretching sheet, radiation, variable viscosity and conductivity), Shawky (2012) (Casson fluid, stretching sheet), Husnain et al. (2012a, b) (unsteady flow, variable viscosity and conductivity), Motsa and Shateyi (2012), Shateyi and Motsa (2012b) (unsteady flow, stretching sheet, chemical reaction, radiation, suction/injection), Chand and Kumar (2012) (viscoelastic fluid, oscillation, slip), Srinivasacharya et al. (2014) (cross-diffusion, stratification), Ahmed et al. (2013a, b) (cross-diffusion, oscillating plate), Anjalidevi and Kyalvizhi (2013) (stretching sheet, radiation, heat source), Das (2013) (moving surface, chemical reaction), Rubio Hernandez and Zueco (2013) (network numerical analysis of radiation absorption and chemical effects for unsteady flow), Harish Babu and Satya Narayana (2013) (variable permeability, micropolar fluid, moving plate), Hussaini et al. (2013) (unsteady flow, variable suction), Prakash et al. (2013) (cross-diffusion, radiation, unsteady flow), Rath et al. (2013) (chemical reaction, periodic permeability), Zafariyan et al. (2013) (secondary effects) Salem (2013) (micropolar fluid, chemical reaction, stretching sheet), Ali et al. (2013a, b), Ganghadhar and Bhaskar Reddy (2013) (chemical reaction, moving plate with suction), Mishra et al. (2013) (viscoelastic fluid, oscillatory suction, and heat source), Ali and Alam (2014) (cross-diffusion, stretching sheet, heat generation), Govindarajan et al. (2014), (chemical reaction, unsteady flow, heat sink), Pal and Mondal (2014c) (cross-diffusion, radiation, stretching sheet, radiation, viscous dissipation), Ramaprasad and Varma (2014) (chemical reaction, heat generation, radiation, unsteady flow), Sarma et al. (2014) (rotation, moving plate), Hsiao et al. (2014) (cross-diffusion, thermophoretic particle deposition), Malga and Kishan (2014) (polar fluid, unsteady flow), Raju and Varma (2014) (cross-diffusion), Ojjela and Naresh Kumar (2014) (cross-diffusion, couple-stress fluid, chemical reaction, Hall and ion slip effects), Seth et al. (2015c) (rotation, radiation, moving plate, heat absorption), Mohanty et al. (2015) (micropolar fluid, stretching sheet), Choudhury and Das (2014) (viscoelasticity, chemical reaction, radiation), Seth and Sarkar (2015) (rotation, chemical reaction, radiation, moving plate), Seth et al. (2015a, b, c) (rotation, moving plate), Pattnaik et al. (2015) (radiation, accelerated plane), Anand Rao et al. (2015) (cross-diffusion, radiation, heat source, unsteady flow), Khan et al. (2015f) (radiation, unsteady flow), Loganathan and Sivapoornapriya (2014b) (impulsively started plate), Mahanta and Shaw (2015) (double diffusion, Casson fluid, unsteady flow, convective boundary condition), Swain and Senapati (2015) (radiation, impulsively started plate), Singh and Kumar (2015) (micropolar fluid, chemical reaction, double stratification), Marneni et al. (2015) (ramped wall temperature, cross-diffusion), Mabood

et al. (2016a) (cross-diffusion, stretching sheet, micropolar fluid, radiation), Prakash et al. (2016a, b, c) (cross-diffusion, radiation, chemical reaction), Uddin et al. (2016b) (stretching sheet, velocity, and thermal slip), Loganathan and Sivapoornapriya (2016a) (viscous dissipation), Madhava Reddy et al. (2016) (cross-diffusion, stratification, impulsively started plate), Seth et al. (2016a, b) (ramped plate temperature, radiation, and either chemical reaction or rotation, heat absorption, and an accelerated plate), Ibrahim and Suneetha (2016) (Soret effect, heat source, chemical reaction, viscous dissipation), Sarma and Pandit (2016) (Soret effect, accelerated plate, rotation about a normal to the plate), Uddin et al. (2016g) (multiple slips, variable properties), Zhao et al. (2016a, b) (fractional Maxwell fluid, cross-diffusion), Singh et al. (2016) (rotation, exponentially accelerated plate) and Mabood and Ibrahim (2016) (stretching sheet, cross-diffusion, micropolar fluid, radiation).

For a horizontal surface, Moorthy et al. (2013) studied cross-diffusion and variable viscosity effects. For an inclined plane, studies were made by Ferdows et al. (2009a, b), Reddy and Reddy (2011), Pal and Chatterjee (2013) (cross-diffusion, power-law fluid, variable conductivity), Uddin and Enamul Karim (2013) (cross-diffusion, heat generation, thermophoresis), Ali et al. (2013a, b) (conjugate effects), and Ismail et al. (2014) (rotation, unsteady flow).

The effects of MHD, radiation, and variable viscosity on convection from a vertical truncated cone were studied by Mandy et al. (2010). Flow past a sphere with cross-diffusion was investigated by Vasu et al. (2012). Stagnation point flow past a horizontal cylinder with radiation was studied by Uddin and Kumari (2011).

9.2.1.2 Non-Newtonian Fluid

A power-law non-Newtonian fluid was studied by Jumar and Majumdar (2000, 2001), Cheng (2006c, 2011b) (yield stress, cross-diffusion), Cheng (2007a, c, 2009a) (vertical wavy surface), El-Hakiem (2009a) (radiation), Ibrahim et al. (2010) (yield stress), Hirata et al. (2010) (yield stress, chemical reaction, cross-diffusion), Narayana et al. (2009a) (yield stress, cross-diffusion), Tai and Char (2010) (cross-diffusion, radiation), Srinivasacharya and Swamy Reddy (2012a, b, 2013a, b, c) (cross-diffusion, chemical reaction, radiation, stratification), Narayana et al. (2009b, 2013b) (cross-diffusion, stratification), and Murthy and Kairi (2009) (cross-diffusion, melting), and Yih and Huang (2015) (internal heating).

A viscoelastic fluid was treated by Choudhury and Dey (2010) (periodic permeability), Salem (2006b) (cross-diffusion), and Malashetty et al. (2012a) (local thermal nonequilibrium). Flow of a viscoelastic fluid over a vertical cone and a flat plate was examined by Kumar and Sivaraj (2013). A polar fluid with chemical reaction and internal heat generation was studied by Patil and Kulkarni (2008) (for a comment, pointing out an error in modeling viscous dissipation, see Rees (2009a)). A micropolar fluid was studied by Chamkha et al. (2004a, b, c) (chemical reaction) and Rashad et al. (2014a) (chemical reaction, radiation). A couple-stress fluid was

investigated by Malashetty et al. (2012b) (cross-diffusion). A Casson fluid was examined by Benazir et al (2016) (magnetic field).

9.2.1.3 Cross-Diffusion

For a vertical wall, cross-diffusion was also studied by Partha et al. (2006, 2008, 2009), Postelnicu (2007c, 2010a) (chemical reaction, stagnation point flow), Tsai and Huang (2009a), El-Arabawy (2009), Rathish Kumar and Krishna Murthy (2010b, 2012b) (wavy boundary, double stratification), Awad et al. (2011a, b) (radiation), Murthy and El-Amin (2011) (stratification), Moorthy and Seethilvadivu (2012a) (variable viscosity), and El-Kabeir et al. (2015a, b) (moving plate, chemical reaction).

Cheng (2012d) studied cross-diffusion with an inclined plate. El-Kabeir (2011) examined cross-diffusion with a stretching cylinder and chemical reaction. Rashad and Chamkha (2014) treated cross-diffusion about a truncated cone.

9.2.1.4 Moving Surface, Stretching Sheet

For a regular porous medium, a moving surface such as a stretching sheet does not have a significant effect in the bulk of the medium. Nevertheless a large number of theoretical papers on this topic have been published, and these we briefly mention.

Flow over a stretching sheet was studied by Abel and Ueera (1998), Abel et al. (2001) (viscoelastic fluid), Salem (2006b) (viscoelastic fluid), Mansour et al. (2008a, b) (chemical reaction, thermal stratification, MHD, cross-diffusion), Aly et al. (2011) (cross-diffusion), Beg et al. (2009a) (MHD, cross-diffusion), Elbashbeshy et al. (2010) (unsteady flow, heat source/sink, variable heat flux), Pal and Chaterjee (2010) (MHD, micropolar fluid, nonuniform heat source, thermal radiation), Pal and Mondal (2010b) (MHD, radiation), Pal and Mondal (2012b) (MHD, Forchheimer drag, nonuniform heat source/sink, variable viscosity), Abdou (2010) (temperature-dependent viscosity), Rahman and Al-Lawatia (2010) (chemical reaction, micropolar fluid), Chamkha et al. (2010b) (unsteady flow, chemical reaction), Kandasamy et al. (2010a) (thermophoresis, temperature-dependent viscosity), Chamkha and Aly (2011) (stagnation point flow, polar fluid, cross-diffusion), Huang et al. (2011) (inclined surface, chemical reaction), Rahman (2012) (chemical reaction, heat generation, variable viscosity and conductivity), Hayat et al. (2015c) (cross-diffusion, exponential stretching, chemical reaction, heat source), and Baoku et al. (2015) (viscoelastic second-grade fluid).

9.2.1.5 Horizontal or Inclined Wall

Li and Lai (1998), Bansod (2003), and Bansod et al. (2005) examined convection from horizontal plates. Also for a horizontal plate, Wang et al. (2003b) obtained an

analytical solution for Forchheimer convection with surface mass flux and thermal dispersion effects, Bansod and Jadhav employed an integral treatment, while Narayana and Murthy (2008), Murthy and Narayana (2010), and Narayana et al. (2012b) studied the effect of cross-diffusion. Triple diffusion along a horizontal plate with a convective boundary condition was investigated by Khan et al. (2014c). For an inclined wall, Durga Prasad et al. (2016) investigated cross-diffusion with a magnetic field. Jhansi Rani et al. (2015) considered a magnetic field and an impulsively started plate while Choudhury and Das (2016) treated a viscoelastic fluid, a magnetic field, and a chemical reaction. A moving vertical cylinder was examined by Loganathan and Eswari (2016).

9.2.1.6 Wavy Surface

Convection over a wavy vertical plate or cone was studied by Cheng (2000c, d), Rathish Kumar and Shalini (2004b), Narayana and Sibanda (2010) (cross-diffusion), and Krishna Murthy et al. (2011) (cross-diffusion). Convection from a wavy wall in a thermally stratified enclosure with mass and thermal stratification was treated numerically by Rathish Kumar and Shalini (2005a, b). A vertical wavy wall with double stratification was also studied by Neagu (2011).

An inclined wavy surface was treated by Cheng (2010b). A corrugated surface with cross-diffusion was studied by Rathish Kumar and Krishna Murthy (2010b). A vertical wavy cone with cross-diffusion was examined by Cheng (2011a).

9.2.1.7 Cone or Wedge or Cylinder or Sphere

A cone, truncated or otherwise, with variable wall temperature and concentration was analyzed by Yih (1999a, d) and Cheng (2000a). For a cone or wedge, convection was treated by Chamkha et al. (2000). A cylinder or a cone with heat generation or absorption effects was examined by Chamkha and Quadri (2001, 2002).

A vertical cone was also treated by Kumari and Nath (2009a), Awad et al. (2011a, b) (cross-diffusion), and Cheng (2009c, d, f, 2010d, 2011a) (non-Newtonian fluid, cross-diffusion, variable wall temperature and concentration, variable wall heat and mass fluxes), Kairi (2011) (power-law fluid), Mahmoud (2013) (non-Newtonian fluid, chemical reaction, heat generation, radiation, variable viscosity), Kairi and Ramreddy (2014), (power-law fluid), Khan and Sultan (2015) (double diffusion, Eyring-Powel fluid) and Benazir et al. (2016) (Casson fluid, magnetic field). A truncated cone was studied by Chamkha et al. (2006b) (icy water), Cheng (2007c) (nonsimilar solutions), Cheng (2007c, 2008, 2009b, e, 2010a) (non-Newtonian fluid, wavy wall, variable viscosity), Mahdy (2010a, b) (chemical reaction, variable viscosity), Kairy and Murthy (2011) and Uddin et al. (2016e) (rotation, anisotropy, slip).

A vertical cylinder was studied by Yücel (1990). Convection above a near-horizontal surface and convection along a vertical permeable cylinder were

analyzed by Hossain et al. (1999a, b). A vertical cylinder was also treated by Cheng (2010c), El-Aziz (2007) (MHD, permeable surface), Singh and Chandarki (2009), Chamkha et al. (2011c), and Reddy (2014a) (radiation, magnetic field). Flow over a slender body of revolution was studied by Lai et al. (1990b). Non-Darcy effects on flow over a two-dimensional or axisymmetric body were treated by Kumari et al. (1988a, b), while Kumari and Nath (1989c, d) dealt with the case where the wall temperature and concentration vary with time. A numerical study of convection in an axisymmetric body was reported by Nithiarasu et al. (1997b).

Flow over a horizontal cylinder, with the concentration gradient being produced by transpiration, was studied by Hassan and Mujumdar (1985). A horizontal permeable cylinder was considered by Yih (1999f). Flow over a horizontal cylinder was also studied by El-Kabeir et al. (2008a, b) (MHD, cross-diffusion, non-Newtonian fluid), Zueco et al. (2009a), Prasad et al. (2012b) (magnetic field, radiation, variable viscosity), and Prasad et al. (2013b) (cross-diffusion). Flow over an elliptical horizontal cylinder was treated by Cheng (2006a, 2011b).

Flow over a wedge with a chemical reaction was investigated by Kandasamy and Palanima (2007), Kandasamy et al. (2008a), and Muhaimin et al. (2009a, b) (MHD, mixed convection, thermophoresis).

The case of a heated sphere was analyzed by Lai and Kulacki (1990a), Ganapathy (2012), and Prasad et al. (2012a) (magnetic field, radiation, variable porosity).

9.2.1.8 Other Situations

A doubly stratified medium was studied by Narayana and Murthy (2006), Rathish Kumar and Shalini (2005a, b) (wavy boundary), Srinivasacharya and RamReddy (2010), and Srinivasacharya et al. (2011). Convection past a curved surface with variable permeability was treated by Mohammadein and Al Shear (2011). Aziz et al. (2014) treated boundary layer slip. Cao and Cui (2015) studied a case in which viscosity, thermal conductivity, and mass diffusivity were power-law functions. The effect of melting on convection about an axisymmetric stagnation point with cross-diffusion and temperature-dependent viscosity was studied by Modather et al. (Sect. 9.2.1).

9.2.2 Enclosed Porous Medium: Channel or Box

As the simplest configuration of simultaneous heat and mass transfer in an enclosed porous medium consider the two-dimensional system defined in Fig. 9.7. The uniform temperature and concentration are maintained at different levels along the two side walls. The main engineering challenge is the calculation of the overall heat and mass transfer rates expressed by Eq. (9.44).

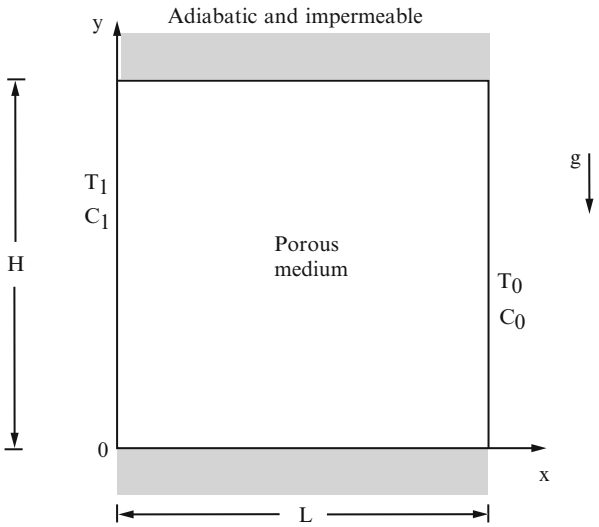

Fig. 9.7 Enclosed porous medium subjected to heat and mass transfer in the horizontal direction

Relative to the single-wall problem (Fig. 9.5) the present phenomenon depends on the geometric aspect ratio L/H as an additional dimensionless group next to N and Le. These groups account for the many distinct heat and mass transfer regimes that can exist. Trevisan and Bejan (1985) identified these regimes on the basis of scale analysis and numerical experiments. Figure 9.8 shows that in the case of heat transfer-driven flows ($|N| << 1$) there are five distinct regimes, which are labeled I–V. The proper Nu and Sh scales are listed directly on the [Le, $(L/H)^2$Ra] subdomain occupied by each regime.

Five distinct regimes also are possible in the limit of mass transfer-driven flows, $|N| >> 1$. Figure 9.9 shows the corresponding Nusselt and Sherwood number scales and the position of each regime in the plane [Le, $(L/H)^2$ Ra$|N|$]. Had we used the plane [Le^{-1}, $(L/H)^2$ Ra$|N|$ Le] then the symmetry with Fig. 9.8 would have been apparent. The Nu and Sh scales reported in Figs. 9.8 and 9.9 are correct within a numerical factor of order 1. Considerably more accurate results have been developed numerically and reported in Trevisan and Bejan (1985).

The most striking effect of varying the buoyancy ratio N between the extremes represented by Figs. 9.8 and 9.9 is the suppression of convection in the vicinity of $N = -1$. In this special limit, the temperature and concentration buoyancy effects are comparable in size but have opposite signs. Indeed, the flow disappears completely if Le $= 1$ and $N = -1$. This dramatic effect is illustrated in Fig. 9.10, which shows how the overall mass transfer rate approaches the pure diffusion level (Sh $= 1$) as N passes through the value -1.

When the Lewis number is smaller or greater than 1, the passing of N through the value -1 is not accompanied by the total disappearance of the flow. This aspect is illustrated by the sequence of streamlines, isotherms, and concentration lines displayed in Fig. 9.11. The figure shows that when N is algebraically greater than approximately -0.85, the natural convection pattern resembles the one that would

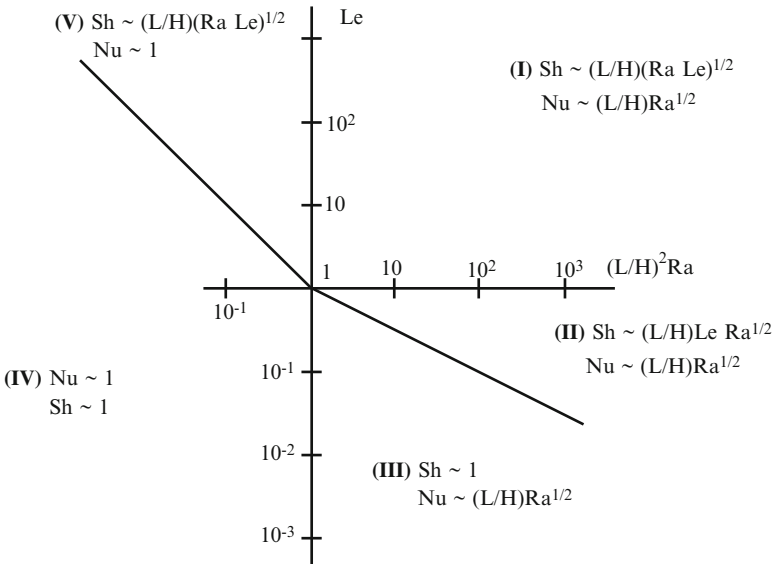

Fig. 9.8 The heat and mass transfer regimes when the buoyancy effect in the system of Fig. 9.7 is due mainly to temperature gradients, $|N| \ll 1$ (Trevisan and Bejan 1985)

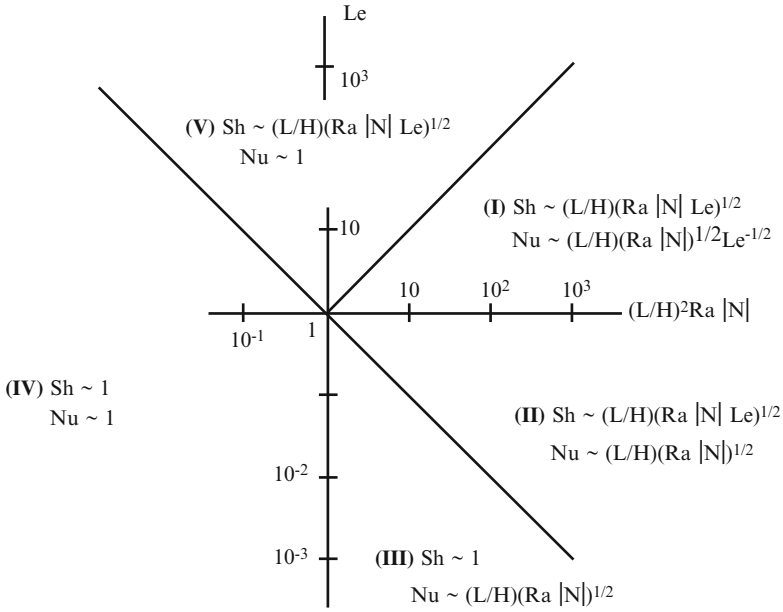

Fig. 9.9 The heat and mass transfer regimes when the buoyancy effect in the system of Fig. 9.7 is due mainly to concentration gradients, $|N| \gg 1$ (Trevisan and Bejan 1985)

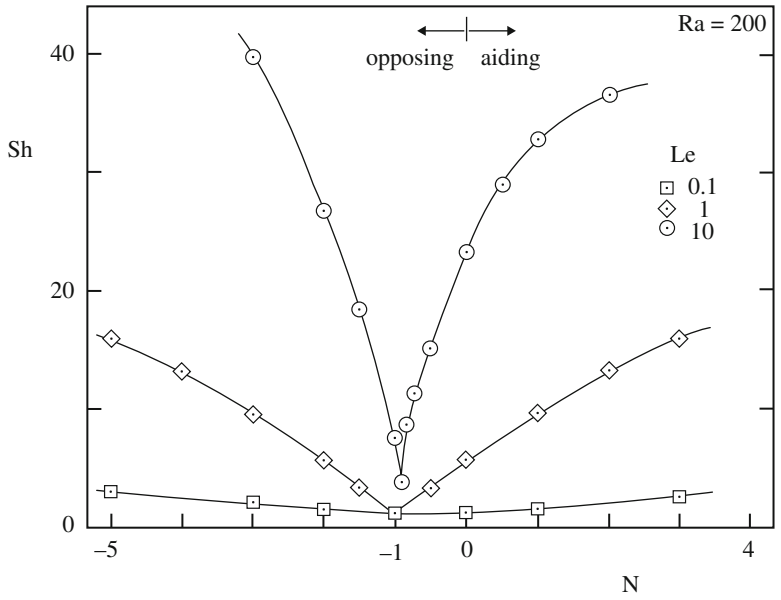

Fig. 9.10 The effect of the buoyancy ratio on the overall mass transfer rate through the enclosed porous medium shown in Fig. 9.7 (Ra = 200, $H/L = 1$) (Trevisan and Bejan 1985)

be expected in a porous layer in which the opposing buoyancy effect is not the dominant driving force. The circulation is reversed at N values lower than approximately -1.5. The flow reversal takes place rather abruptly around $N = -0.9$, as is shown in Fig. 9.11b. The core, which exhibited temperature and concentration stratification at N values sufficiently above and below -0.9, is now dominated by nearly vertical constant T and C lines. This feature is consistent with the tendency of both Nu and Sh to approach their pure diffusion limits (e.g., Fig. 9.10).

A compact analytical solution that documents the effect of N on both Nu and Sh was developed in a subsequent paper by Trevisan and Bejan (1986). This solution is valid strictly for Le = 1 and is based on the constant-flux model according to which both sidewalls are covered with uniform distributions of heat flux and mass flux. The overall Nusselt number and Sherwood number expressions for the high Rayleigh number regime (distinct boundary layers) are

$$\mathrm{Nu} = \mathrm{Sh} = \frac{1}{2}\left(\frac{H}{L}\right)^{1/5} \mathrm{Ra}_*^{2/5}(1+N)^{2/5}, \tag{9.52}$$

where Ra_* is the heat flux Rayleigh number defined by $\mathrm{Ra}_* = g\beta KH^2 q''/\nu\alpha_m k_m$. These theoretical Nu and Sh results agree well with numerical simulations of the heat and mass transfer phenomenon.

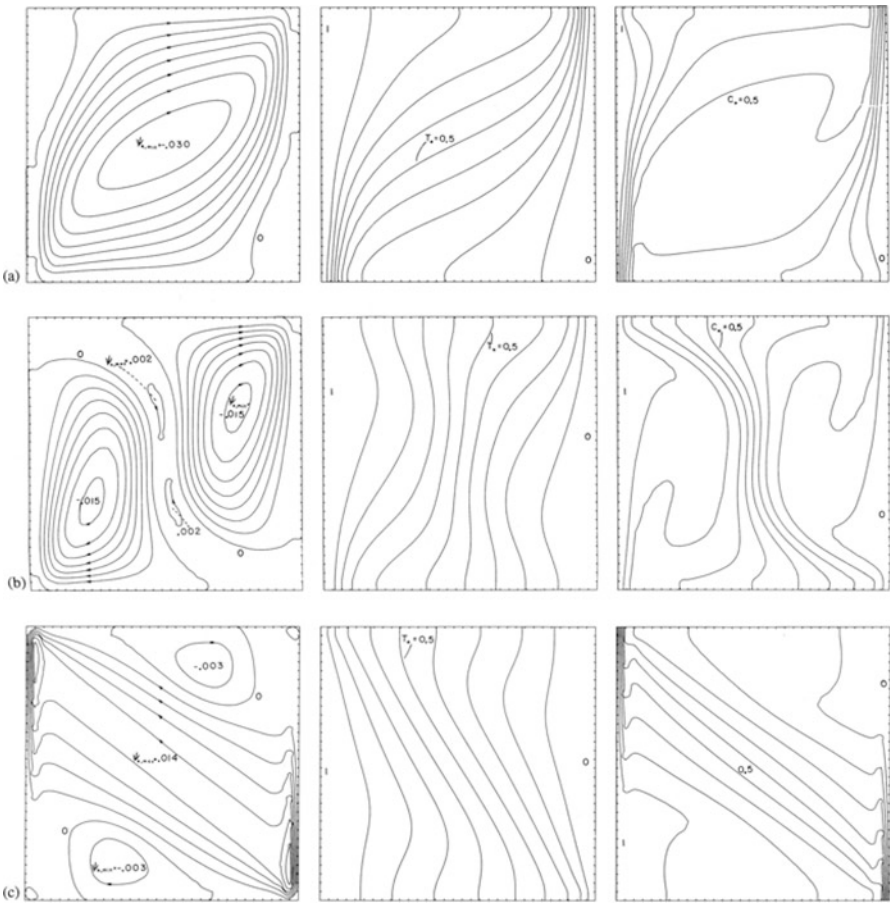

Fig. 9.11 Streamlines, isotherms, and isosolutal lines for natural convection in the enclosed porous medium of Fig. 9.7, showing the flow reversal that occurs near $N = -1$ (Ra = 200, Le = 10, $H/L = 1$). (**a**) $N = -0.85$; (**b**) $N = -0.9$; and (**c**) $N = -1.5$ (Trevisan and Bejan 1985)

Another theoretical result has been developed by Trevisan and Bejan (1986) for the large Lewis numbers limit in heat transfer-driven flows ($|N| << 1$). In this limit the concentration boundary layer can be described by means of a similarity solution, leading to the following expression for the overall Sherwood number:

$$\mathrm{Sh} = 0.665\left(\frac{L}{H}\right)^{1/10} \mathrm{Le}^{1/2}\mathrm{Ra}_*^{3/10}. \tag{9.53}$$

The mass flux j used in the Sh definition, $\mathrm{Sh} = jH/D_\mathrm{m}\,\Delta C$, is constant, while ΔC is the resulting concentration-temperature difference between the two sidewalls. Equation (9.53) is also in good agreement with numerical experiments.

It has been shown that the constant-flux expressions (9.52) and (9.53) can be recast in terms of dimensionless groups (Ra, Nu, Sh) that are based on temperature and concentration differences. This was done in order to obtain approximate theoretical results for the configuration of Fig. 9.7, in which the sidewalls have constant temperature and concentrations (Trevisan and Bejan 1986). Similarly, appropriately transformed versions of these expressions can be used to anticipate the Nu and Sh values in enclosures with mixed boundary conditions, that is, constant T and j, or constant q'' and C on the same wall. Numerical simulations of the convective heat and mass transfer across enclosures with mixed boundary conditions are reported by Trevisan and Bejan (1986).

An analytical and numerical study of convection in vertical slots due to prescribed heat flux at the vertical boundaries was made by Alavyoon (1993), whose numerical results showed that of any value of $\mathrm{Le} > 1$ there exists a minimum aspect ratio A below which the concentration field in the core region is rather uniform and above which it is linearly stratified in the vertical direction. For $\mathrm{Le} > 1$ the thermal layers at the top and bottom of the enclosure are thinner than their solutal counterparts. In the boundary layer regime and for sufficiently large A the thicknesses of the vertical boundary layers of velocity, concentration, and temperature were found to be equal. The case of opposing fluxes was studied by Alavyoon et al. (1994). They found that at sufficiently large values of Ra, Le, and A there is a domain of N in which one obtains oscillating convection, while outside this domain the solution approaches steady-state convection.

Numerical simulations based on an extension to the Brinkman model for the case of cooperating thermal and solutal buoyancy forces in the domain of positive N and for $\mathrm{Le} > 1$ were reported by Goyeau et al. (1996a). The Brinkman model was also employed by Mamou et al. (1998a).

The studies reviewed in this subsection are based on the homogeneous and isotropic porous medium model. The effect of medium heterogeneity on the heat and mass transfer across an enclosure with constant-flux boundary conditions is documented by Mehta and Nandakumar (1987). They show numerically that the Nu and Sh values can differ from the values anticipated based on the homogeneous porous medium model.

For the case $N = -1$, a purely diffusive solution exists for suitable geometry and boundary conditions. Charrier-Mojtabi et al. (1997, 1998) have studied this case for a rectangular slot with constant temperature imposed on the side walls. The onset of convection for which $\gamma = \mathrm{Le}\theta$ occurs when $\mathrm{Ra}\,|\mathrm{Le} - 1|$ exceeds a certain critical value, depending on the aspect ratio A. The critical value is 184.06 for a square cavity ($A = 1$) and 105.33 for a vertical layer of infinite extent; the corresponding critical wavenumber has the value 2.51. For $A = 1$, they also performed numerical simulations, the results of which confirmed the linear instability results. They observed that the bifurcation to convection was of the transcritical type and that the bifurcation diagrams indicated the existence of both symmetrical and asymmetrical subcritical and supercritical solutions.

A numerical study for a square cavity, comparing the Darcy, Forchheimer, and Brinkman models, was made by Karimi-Fard et al. (1997). They found that Nu and

Sh increase with Da and decrease with increase of a Forchheimer parameter. The quadratic drag effects are almost negligible, but the boundary effect is important. A further numerical study, for the case of opposing buoyancy effects, was reported by Angirasa and Peterson (1997a). Effects of porosity variation were emphasized in the numerical study by Nithiarasu et al. (1996). Three-dimensional convection in a cubic or rectangular enclosure with opposing horizontal gradients of temperature and concentration was studied numerically by Sezai and Mohamad (1999) and Mohamad and Sezai (2002). A numerical treatment with a random porosity model was reported by Fu and Ke (2000).

The various studies for the case $N = -1$ have demonstrated that there exists a threshold for the onset of monotonic convection, such that oscillatory convection occurs in a narrow range of values of Le (close to 1, applicable for many gases) depending on the normalized porosity. For the case of an infinite layer, the wavelength at the onset of stationary convection is independent of the Lewis number but this is not so for overstability. When the Lewis number is close to unity the system remains conditionally stable provided that the normalized porosity is less than unity. For a vertical enclosure with constant heat and solute fluxes, the particular case $N = -1 + \varepsilon$ case (where ε is a very small positive number) was studied by Amahmid et al. (2000). In this situation multiple unicellular convective flows are predicted.

A non-Newtonian fluid was studied theoretically and numerically by Getachew et al. (1998) and by Benhadji and Vasseur (2003), and by Ben Khelifa et al. (2012). El-Sayed et al. (2011) studied the effect of chemical reaction with a non-Newtonian fluid in a vertical peristaltic tube. Convection in a couple-stress fluid in a horizontal wavy channel was investigated by Muthuraj et al. (2013).

An electrochemical experimental method was demonstrated by Chen et al. (Chen et al. 1999a, b). An inverse method, leading to the determination of an unknown solute concentration on one wall given known conditions for temperature and concentration on the remaining faces, was reported by Prud'homme and Jiang (2003).

A cavity with a freely convecting wall was studied by Nithiarasu et al. (1997c). The case of constant heat and mass fluxes was investigated by Masuda et al. (1997). A numerical study of the effect of thermal stratification on convection in a square enclosure was made by Rathish Kumar et al. (2002). Convection in a square cavity, or a horizontal layer with the Soret effect included, under crossed heat and mass fluxes was studied analytically and numerically by Bennacer et al. (2001a, 2003b). Entropy production in a square cavity was treated by Mchirgui et al. (2012). Convection in a vertically layered system, with a porous layer between two clear layers, was studied by Mharzi et al. (2000). Anisotropic cavities were studied analytically and numerically by Tobbal and Bennacer (1998), Bera et al. (1998, 2000), Bera and Khalili (2002a), and Muasovi and Shahnazari (2008). Explicit algebraic analytical solutions were presented by Cai et al. (2003) and Cai and Liu (2008). The effect of a magnetic field was studied by Robillard et al. (2006) and Ahmed and Zueco (2011) (rotation, Hall current). Akbal and Baytas (2008) investigated the effects of nonuniform porosity on convection in a cavity with a partly

permeable wall. A cavity with icy water was studied by Kandasamy et al. (2008a), Sivasankaran et al. (2008), and Eswaramurthi and Kandaswamy (2009). Unusual oscillations in a box with opposing heat and mass fluxes on the vertical walls were investigated numerically by Masuda et al. (2008, 2010, 2013). A box subjected to heat and mass fluxes was studied analytically and numerically by Bennisaad and Ouazaa (2012)A heterogeneous cavity was examined by Choukairy and Bennacer (2012). Mimouni et al. (2014) studied two- and three-dimensional transitions in an elongated horizontal enclosure. A shallow cavity heated and salted from the sides with cross-diffusion was studied by Alloui and Vasseur (2013a). They found multiple solutions when the buoyancy ratio is close to unity. A cavity with partly active vertical walls was studied by Jena et al. (2013a). A highly accurate numerical solution for Brinkman convection in a box was reported by Shao et al. (2016). Triple diffusion in a square cavity was studied by Ghalambaz et al. (2016).

Unsteady convection in a box with nonuniform boundary conditions was investigated by Mondal and Sibanda (2015). Three-dimensional convection in a cubic box was examined by Amel et al. (2014) and Hadidi et al. (2016) (partly filled layer). Local thermal nonequilibrium was investigated by Bousri et al. (2012) (chemical reaction) and Bera et al. (2014) (square cavity). An anisotropic box with nonuniform temperature and concentration on the lower wall was studied by Kumar et al. (2015d). For horizontal rectangular enclosures and heterogeneous media, with the horizontal and vertical walls subject to different mass and heat transfer, Choukairy et al. (2016) discussed the limitation of the 2D parallel flow assumption for 2D-3D transition. A rectangular box with walls partly thermally active was studied by Saberi and Nikbakhti (2016).

Analytical and numerical studies of convection in a vertical layer were reported by Amahmid et al. (1999b, c, 2000, 2001), Bennacer et al. (2001b), Mamou et al. (1998a), and Mamou (2002a). A vertical layer or slot was also treated by Asbik et al. (2002) (evaporation), Mharzi et al. (2002) (vertical layering), Dash et al. (2010) (second-order fluid), Li et al. (2006b) (transient convection, gas diffusion), Rawat et al. (2009) (transient convection, MHD, micropolar fluid, variable thermal conductivity, heat source), Zhao et al. (2007b) (thermal and solutal source), Liu et al. (2008b) (concentrated energy and solute sources), Er-Raki et al. (2010) (cross-diffusion), Kheilifa et al. (2012) (non-Newtonian fluid), Kumar et al. (2013b) (micropolar fluid, magnetic field, radiation), Harzallah et al. (2014), (walls of finite thickness, anisotropy, local thermal nonequilibrium), Manglesh et al. (2014), (cross-diffusion, magnetic field), Umavathi (2015a, b, c) (chemical reaction, variable viscosity and conductivity), Mathew and Singh (2015) (span-wise fluctuation, radiation, chemical reaction), Ojjela and Naresh Kumar (2016) (unsteady MHD flow, cross-diffusion, chemical reaction, couple-stress fluid) Usman et al. (2016) (radiation, slip condition), Doh et al. (2016) (micropolar fluid, transient flow, boundary conditions of the third kind), and Reddy et al. (2016a, b, c) (magnetic field, rotation, viscoelastic fluid, radiation). An inclined box was studied by Chandra Shekhar and Kishan (2015) (cross-diffusion), Abdelkrim and Mahfoud (2014), Kefayati (2016a, b) (cross-diffusion, power-law fluid), and Mondal and Sibanda (2016) (unsteady flow, radiation). For a vertical asymmetric channel and a

Maxwell fluid, cross-diffusion, radiation, and chemical reaction, Noreen and Saleem (2016) investigated peristaltic flow. Aly (2016a) and Aly and Asai (2016) used the incompressible smooth particle hydrodynamic numerical method to study an enclosure containing a sloshing rod and also an annulus or enclosure with cross-diffusion and anisotropy. A numerical study within a horizontal partly porous enclosure was made by Hadidi et al. (2016). Unsteady convection in an inclined rectangular enclosure was investigated by Mondal and Sibanda (2016b).

9.2.3 Transient Effects

Another basic configuration in which the net heat and mass transfer occurs in the horizontal direction is the time-dependent process that evolves from a state in which two (side-by-side) regions of a porous medium have different temperatures and species concentrations. In time, the two regions share a counter-flow that brings both regions to a state of thermal and chemical equilibrium. The key question is how parameters such as N, Le, and the height-length ratio of the two-region ensemble affect the time scale of the approach to equilibrium. These effects have been documented both numerically and on the basis of scale analysis by Zhang and Bejan (1987).

As an example of how two dissimilar adjacent regions come to equilibrium by convection, Fig. 9.12 shows the evolution of the flow, temperature, and concentration fields of a relatively high Rayleigh number flow driven by thermal buoyancy effects ($N = 0$). As the time increases, the warm fluid (initially on the left-hand side) migrates into the upper half of the system. The thermal barrier between the two thermal regions is smoothed gradually by thermal diffusion. Figure 9.12c, d show that as the Lewis number decreases the sharpness of the concentration dividing line disappears as the phenomenon of mass diffusion becomes more pronounced.

In the case of heat transfer-driven flows, the time scale associated with the end of convective mass transfer in the horizontal direction is

$$\widehat{t} = \frac{\varphi}{\sigma}\left(\frac{L}{H}\right)^2 \mathrm{Ra}^{-1} \text{ if } \quad \mathrm{LeRa} > \frac{\varphi}{\sigma}\left(\frac{L}{H}\right)^2, \tag{9.54}$$

$$\widehat{t} = \frac{\varphi}{\sigma}\left(\frac{L}{H}\right)^2 \mathrm{Le} \text{ if } \quad \mathrm{LeRa} < \frac{\varphi}{\sigma}\left(\frac{L}{H}\right)^2. \tag{9.55}$$

The dimensionless time $\widehat{t}$ is defined as

$$\widehat{t} = \frac{\alpha_{\mathrm{m}} t}{\sigma H^2}. \tag{9.56}$$

Values of $\widehat{t}$ are listed also on the side of each frame of Fig. 9.12. The time criteria (9.54)–(9.56) have been tested numerically along with the corresponding time

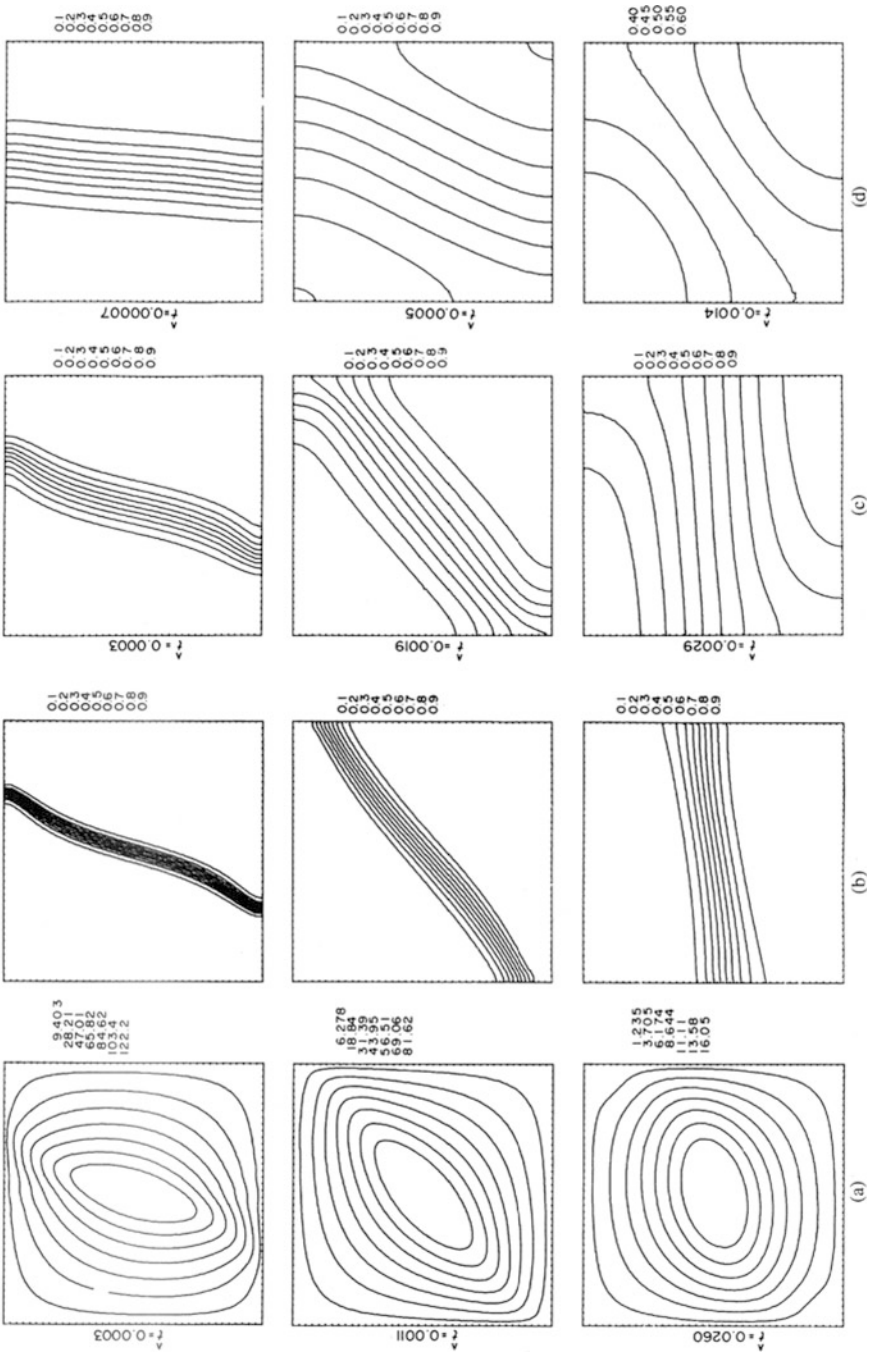

Fig. 9.12 The horizontal spreading and layering of thermal and chemical deposits in a porous medium ($N = 0$, $\mathrm{Ra} = 1000$, $H/L = 1$, $\Phi/\sigma = 1$). (**a**) Streamlines; (**b**) isotherms, or isosolutal lines for $\mathrm{Le} = 1$; (**c**) isosolutal lines for $\mathrm{Le} = 0.1$; and (**d**) isosolutal lines for $\mathrm{Le} = 0.01$ (Zhang and Bejan 1987)

scales for approach to thermal equilibrium in either heat transfer-driven or mass transfer-driven flows.

The transient problem for the case of a vertical plate, with a simultaneous step change in wall temperature and wall concentration, was treated numerically using a Brinkman-Forchheimer model by Jang et al. (1991). They found that the time to reach steady state decreases with increase of Da or magnitude of the buoyancy ratio N, increases with increase of the inertia coefficient c_F, and passes through a minimum as Le increases through the value 1. Earlier Pop and Herwig (1990) had shown that when just the concentration was suddenly changed at an isothermal vertical plate, the local Sherwood number decreases with time and approaches its steady-state value. Cheng (2000b) analyzed a problem involving transient heat and mass transport from a vertical plate on which the temperature and concentration are power functions of the streamwise coordinate. The influence of fluctuating thermal and mass diffusion on unsteady MHD buoyancy-driven convection past a vertical plate with variable wall heat and mass fluxes was studied by Pal and Talukdar (2012a).

Milne and Butler (2007) carried out a numerical investigation of the effects of compositional and thermal buoyancy on transient plumes in a porous layer.

9.2.4 *Stability of Flow*

The stability of the steady Darcy flow driven by differential heating of the isothermal walls bounding an infinite vertical slab with a stabilizing uniform vertical salinity gradient was studied independently by Gershuni et al. (1976, 1980) and Khan and Zebib (1981). Their results show disagreement in some respects. We believe that Gershuni et al. are correct. The flow is stable if $|\mathrm{Ra}_D|$ is less than $\mathrm{Ra_{D1}} = 2.486$ and unstable if $|\mathrm{Ra_D}| > \mathrm{Ra_{D1}}$. The critical wavenumber α_c is zero for $\mathrm{Ra_{D1}} < |\mathrm{Ra_D}| < \mathrm{Ra_{D2}}$ where $\mathrm{Ra_{D2}} \approx 52$ for the case $N = 100$, $\sigma = 1$, and nonzero for $|\mathrm{Ra_D}| > \mathrm{Ra_{D2}}$. As $|\mathrm{Ra_D}| \to \infty$; either monotonic or oscillatory instability can occur depending on the values of N and σ. If, as in the case of aqueous solutions, N and N/σ are fairly large and of the same order of magnitude, then monotonic instability occurs and the critical values are

$$\mathrm{Ra_c} = \frac{2\pi^{1/2}}{|N-1|}|\mathrm{Ra_D}|^{3/4}, \quad \alpha_c = \left(\frac{\pi}{2}\right)^{1/2}|\mathrm{Ra_D}|^{1/4}. \tag{9.57}$$

Mamou et al. (1995a) have demonstrated numerically the existence of multiple steady states for convection in a rectangular enclosure with vertical walls. Mamou et al. (1995b) studied analytically and numerically convection in an inclined slot. Again multiple solutions were found. Convection in an inclined cavity with a temperature-dependent heat source or sink was studied by Chamkha and Al-Mudhaf (2008a, b).

Two-dimensional convection produced by an endothermic chemical reaction and a constant heat flux was examined by Basu and Islam (1996). They identified various routes to chaos. The onset of convection in a rectangular cavity with balanced heat and mass fluxes applied to the vertical walls was analyzed by Marcoux et al. (1999a). An analytical and numerical study of a similar situation was reported by Mamou et al. (1998d).

9.3 Concentrated Heat and Mass Sources

9.3.1 Point Source

Poulikakos (1985a) considered the transient flow as well as the steady flow near a point source of heat and mass in the limit of small Rayleigh numbers based on the heat source strength q[W], $\widetilde{R}a = g\beta Kq/\nu\alpha_m\, k_m$. The relative importance of thermal and solutal buoyancy effects is described by the "source buoyancy ratio"

$$N_s = \frac{\beta_C m/D_m}{\beta q/k_m}, \tag{9.58}$$

in which m[kg/s] is the strength of the mass source.

Figure 9.13 shows Poulikakos' (1985a) pattern of streamlines for the time-dependent regime. The curves correspond to constant values of the special group $\psi_* {t_*}^{-1/2}(1 - N_s)$, in which

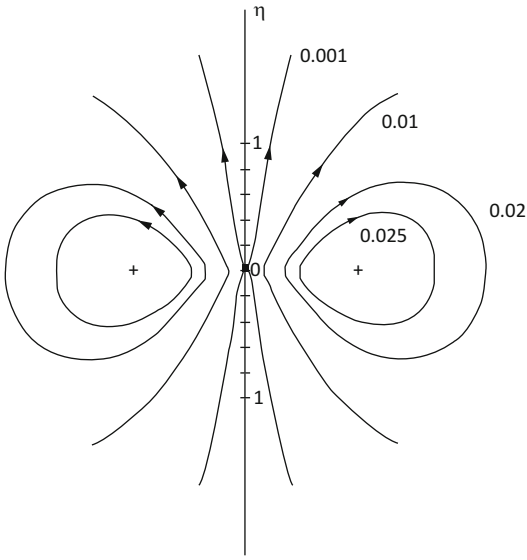

Fig. 9.13 The time-dependent flow field around a suddenly placed point source of heat and mass ($A = 1$) (Poulikakos 1985a, with permission from Pergamon Press)

$$\psi_* = \frac{\psi}{\alpha_m} K^{-1/2}, \quad t_* = \frac{\alpha_m t}{\sigma K}, \tag{9.59}$$

and where $\psi[\mathrm{m}^3/\mathrm{s}]$ is the dimensional streamfunction. The radial coordinate η is defined by

$$\eta = \frac{r}{2}\left(\frac{\sigma}{\alpha_m t}\right)^{1/2}, \tag{9.60}$$

showing that the flow region expands as $t^{1/2}$. Figure 9.13 represents the special case $A = 1$, where A is shorthand for

$$A = \left(\frac{\varphi}{\sigma}\mathrm{Le}\right)^{1/2}. \tag{9.61}$$

Poulikakos (1985a) showed that the A parameter has a striking effect on the flow field in cases where the two buoyancy effects oppose one another ($N_s > 0$ in his terminology). Figure 9.14 illustrates this effect for the case $N = 0.5$ and $A = 0.1$; when A is smaller than 1, the ring flow that surrounds the point source (seen also in Fig. 9.13) is engulfed by a far-field unidirectional flow. The lines drawn on Fig. 9.14 correspond to constant values of the group $2\pi\psi_* t_*^{-1/2}$.

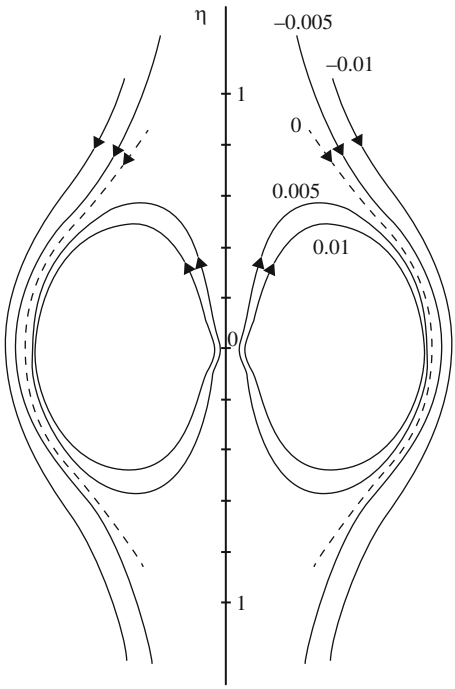

Fig. 9.14 The effect of a small Lewis number (or small A) on the transient flow near a point source of heat and mass ($N = 0.5$, $A = 0.1$) (Poulikakos 1985a, with permission from Pergamon Press)

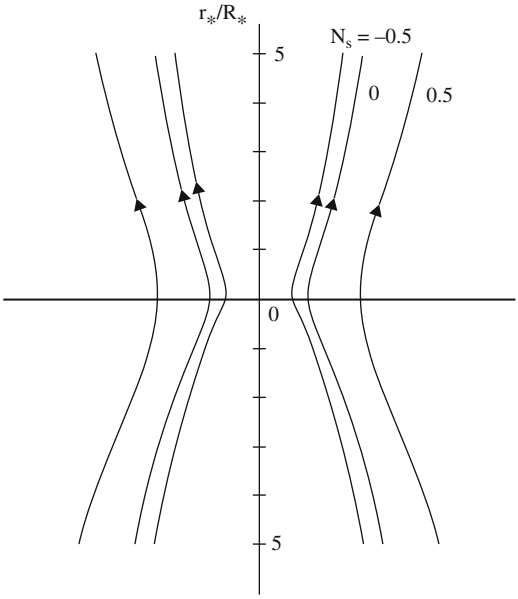

Fig. 9.15 The steady-state flow near a point source of heat and mass ($\widetilde{R}$ a = 5, Le = 1), and the effect of the source buoyancy ratio (Poulikakos 1985a, with permission from Pergamon Press)

In the steady state and in the same small-$\widetilde{R}a$ limit, the flow, temperature, and concentration fields depend only on $\widetilde{R}a$, N_s, and Le. Figure 9.15 shows the migration of one streamline as the buoyancy ratio N_s increases from -0.5 to 0.5, that is, as the buoyancy effects shift from a position of cooperation to one of competition. When the buoyancy effects oppose one another, $N = 0.5$, the vertical flow field is wider and slower. The curves drawn in Fig. 9.15 correspond to $\psi^* = \mathrm{Ra}R^*/8\pi$, where $R^* = R/K^{1/2}$ and R is a reference radial distance. Asymptotic analytical solutions for the steady-state temperature and concentration fields also are reported by Poulikakos (1985a). Ganapathy (1994a) treated the same problem using the Brinkman model. For the case of large Rayleigh numbers, a boundary layer analysis was carried out by Nakayama and Ashizawa (1996). They showed that for large Le the solute diffuses some distance from the plume centerline and the mass transfer influences both velocity and temperature profiles over a wide range. For large Le the solute diffuses within a narrow region along the centerline. A strongly peaked velocity profile then appears for positive buoyancy ratio N, while a velocity defect emerges along the centerline for negative N.

A finite element model for a leaking third species migration from a heat source buried in a porous medium was demonstrated by Nithiarasu (1999). An inverse problem, namely the determination from temperature measurement of an unknown volumetric heat source that is a function of the solute concentration, was discussed by Prud'homme and Jasmin (2003) and Jasmin and Prud'homme (2005). Hill (2005) has considered the linear and nonlinear stability of a layer in which there is a concentration-dependent internal volumetric heat source. Ganapathy and Mohan (2016) studied a concentrated source with cross-diffusion.

9.3.2 Horizontal Line Source

The corresponding heat and mass transfer processes in the vicinity of a horizontal line source were analyzed by Larson and Poulikakos (1986). The source buoyancy ratio in this case is

$$N_s{}' = \frac{\beta_C m'/D_m}{\beta q'/k_m}, \tag{9.62}$$

where q' [W/m] and m' [kg/m/s] are the heat and mass source strengths. All the features described in the preceding sections also are present in the low Rayleigh number regime of the line source configuration. The Rayleigh number for the line source is based on the heat source strength q',

$$\widehat{\mathrm{Ra}} = \frac{g\beta K^{3/2} q'}{\nu \alpha_m k_m}. \tag{9.63}$$

In addition to developing asymptotic solutions for the transient and steady states, Larson and Poulikakos (1986) illustrated the effect of a vertical insulated wall situated in the vicinity of the horizontal line source. An instantaneous point source was treated by Ganapathy (1994a). An analysis using the Brinkman model was reported by Ganapathy (1994b).

The high Rayleigh number regime was studied by Lai (1990a). He obtained a similarity solution and made calculations for a range of Le and N values. For the special case Le = 1 he obtained a closed form solution analogous to that given by Eqs. (5.192)–(5.196). The study of Nakayama and Ashizawa (1996) mentioned in the previous section covered the case of a line source also.

9.4 Other Configurations and Effects

Natural convection in a horizontal shallow layer induced by a finite source of chemical constituent was given a numerical treatment by Trevisan and Bejan (1989).

Convection in a vertical annulus was studied analytically and numerically by Marcoux et al. (1999b) (analytically and numerically), Beji et al. (1999) (who analyzed the effect of curvature on the value of N necessary to pass from clockwise to anticlockwise rolls), Bennacer (2000), Bennacer et al. (2000), (Brinkman model), Benzeghiba et al. (2003) (partly porous annulus), Bahloul et al. (2004b) (separation of components with uniform wall heat fluxes), Bennacer and Lakhal (2005) (thermal diffusion), Cheng (2006a) (asymmetric wall temperatures and concentrations), Bahloul et al. (2006) (tall annulus), Kalita and Dass (2011) (higher order compact simulation), Sankar et al. (2012a, b) (discrete heat and solute source), Sankar et al.

(2012a, b), Badruddin et al. (2012a, b, c), Reddy and Rao (2012) (cross-diffusion, quadratic density variation), Mallikarjuna et al. (2014) (cross-diffusion, heat sources), and Jha et al. (2015e) (cross-diffusion).

A horizontal annulus was treated by Al-Amiri et al. (2006) (pulsating heating), Alloui and Vasseur (2011a, b) (centrifugal force field), Moukalled and Darwish (2013), and Boulechfar and Djezzar (2014) (elliptical annulus) and Abahri et al. (2017) (thermogravitational separation). A rhombic annulus was studied by Moukalled and Darwish (2013, 2015). A thin vertical ring was investigated by Magomedbekov (1997). A rectangular horizontal annulus, with inner/outer walls at high/low temperature and concentration, was studied by Jena et al. (2013b).

A problem involving a vertical enclosure with two isotropic or anisotropic porous layers was studied numerically by Bennacer et al. (2003a), while convection in a partly filled rectangular enclosure was studied numerically by Goyeau and Gobin (1999), Singh et al. (1999), and Younsi et al. (2001). Unsteady convection in a vertical enclosure with radiation was investigated by Jbara et al. (2013a). Thermal enhancement in storage silos (internally heated vertical open-ended cylinders) with periodic wall heating was studied numerically by Himrane et al. (2016).

The onset of convection in an inclined layer has been studied using linear stability analysis and numerically by Karimi-Fard et al. (1998, 1999), who obtained parameter ranges for which the first primary bifurcation is a Hopf bifurcation (oscillatory convection). The same problem was studied numerically by Mamou et al. (1998c) and Mamou (2004) using a finite element method and by Chamkha and Al-Naser (2001) using a finite-difference method. An inclined layer was also investigated by Chamkha and Abdulgafoor (2006), Al-Farhany and Turan (2012), Hadidi et al. (2013, 2015) (bi-layered), Chamkha et al. (2011b), Mchirgui et al. (2014) (second law analysis), and Rtibi et al. (2013, 2014) (cross-diffusion), Chamkha and Al-Mudhaf (2008a, b) studied inclined cavities with various aspect ratios, with a temperature-dependent source or sink, and Siavashi et al. (2017) (entropy generation, various source configurations).

The composite fluid layer over a porous substrate was studied theoretically by Chen (1990), who extended to a range of Ra_m (the thermal Rayleigh number in the porous medium as defined in Eq. (6.167)) the calculations initiated by Chen and Chen (1988c) for the salt-finger situation. For small $\mathrm{Ra_m}$ (=0.01) there is a jump in α_c as the depth ratio $\widehat{d} = d_\mathrm{f}/d_\mathrm{m}$ increases (the jump is fivefold as $\widehat{d}$ increases between 0.2 and 0.3). For large $\mathrm{Ra_m}$ (=1) there is no sudden jump. Convection occurs primarily in the fluid layer if $\widehat{d}$ is sufficiently large. When this is so, multicellular convection occurs for sufficiently large $\mathrm{Ra_m}$. The cells are superposed and their number increases with increase of $\mathrm{Ra_m}$. For $\widehat{d} < 0.1$, the critical $\mathrm{Ra_{Dm}}$ (the solutal Rayleigh number for the porous medium layer) and α_cm decrease as $\widehat{d}$ increases, but when multicellular convection occurs the critical $\mathrm{Ra_{Dm}}$ remains almost constant as $\widehat{d}$ is increased for fixed $\mathrm{Ra_m}$. Zhao and Chen (2001) returned to the same problem but used a one-equation model rather than a two-equation model. They found that the two models predicted quantitative differences in the critical conditions and flow streamlines at the onset of convection, and they noted that carefully conducted

experiments were needed to determine which model gave the more realistic results. A further study of the composite problem was conducted by Gobin and Goyeau (2012) in the context of a general discussion of the validity of one-domain and two-domain approaches. A vertical composite channel with a wavy interface was studied by Mehdaoui et al. (2010). A partly filled horizontal enclosure was examined by Hadidi et al. (2016).

Goyeau et al. (1996b) studied numerically for $N > 0$ the effect of a thin layer of low permeability medium, which suppresses the convective mass transfer. Further numerical studies were reported by Gobin et al. (1998, 2005).

Transient double-diffusive convection in a fluid/porous layer composite was studied by Kazmierczak and Poulikakos (1989, 1991) numerically and then experimentally. The system considered was one containing a linear stabilizing salt distribution initially and suddenly heated uniformly from below at constant flux. In the experiments it was possible to visually observe the flow in the fluid layer but not in the porous layer. In all the experiments $\widehat{d} = 1$, and most of the convective flow took place in the fluid layer. In general, a series of mixed layers formed in turn, starting with one just above the porous layer as time increased, as one would expect if the porous matrix was absent. A corresponding numerical study, with the system cooled through its top boundary (adjacent to the solid layer), was conducted by Rastogi and Poulikakos (1993). A numerical study involving two layers of contrasting permeabilities was conducted by Saghir and Islam (1999). A transient problem involving double-diffusive convection from a heated cylinder buried in a saturated porous medium was studied numerically by Chaves et al. (2005).

An experimental study with a clear liquid layer below a layer at porous medium was performed by Rastogi and Poulikakos (1997). They took the initial species concentration of the porous layer to be linear and stable and that in the clear fluid uniform and the system initially isothermal and then cooled from above. Al-Farhany and Turan (2001) studied a layer bounded by walls of finite thickness. Baytas et al. (2009) treated an enclosure filled by a step type porous layer. Further work on fluid/porous regions was performed by Alloui et al. (2008).

Sandner (1986) performed experiments, using salt water and glass beads in a vertical cylindrical porous bed. In his experiments the salt concentration was initially uniform. When the system was heated at the bottom, a stabilizing salinity gradient developed, due to the Soret effect. Some related work is discussed in Sect. 10.5.

Natural convection in a trapezoidal enclosure was studied numerically by Nguyen et al. (1997a) (anisotropy) and Younsi (2009) (MHD). A forced convection flow around a porous medium layer placed downstream on a flat plate was studied numerically and experimentally by Lee and Howell (1991). Convection in a parallelogrammic enclosure was studied numerically by Costa (2004). A transient problem, involving a smaller rectangular cavity containing initially cold fresh fluid located in the corner of a larger one containing hot salty fluid, was studied numerically by Saghir (1998). Inclined triangular enclosures were studied by Chamkha et al. (2010d) (fins, heat generation/absorption) and Mansour et al.

(2011a) (unsteady convection, heat source/sink, sinusoidal boundary conditions). The effects of MHD, radiation, and variable viscosity on convection from a vertical truncated cone were studied by Mandy et al. (2010). A vertical truncated cone with Soret and Dufour effects was studied by Cheng et al. (2012a). Mansour et al. (2012) studied a square enclosure with unsteady convection and sinusoidal boundary conditions.

Melnikov and Shevtsova (2011) studied separation of a binary fluid in a fluid-porous-fluid system. Srinivasacharya and RamReddy (2011a) treated convection of a doubly stratified micropolar fluid on a vertical wall. Salama (2011b) studied a vertical wall with thermophoresis, radiation, and heat generation. The case of a 2D rectangular cavity with uniform and constant heat and solutal mass fluxes imposed on the horizontal walls and with impermeable and adiabatic vertical walls was studied by Bennisaad and Ouazaa (2012). Ahadi et al. (2014) presented an experimental, theoretical, and numerical interpretation of thermo-diffusion separation for a non-associating binary mixture in liquid/porous layers. Chaves et al. (2015) studied numerically the heat transfer by double diffusion from a heated buried cylinder. A spherical shell used to model the Earth's core was studied by Takahashi (2014). Convection with cross-diffusion from a frustum or wavy cone with nonuniform wall temperature and concentration was examined by Cheng (2015b).

9.5 Inclined and Crossed Gradients

The effects of horizontal gradients on thermosolutal stability, for the particular case where the horizontal thermal and solutal gradients compensate each other as far as density is concerned, was studied theoretically by Parvathy and Patil (1989) and Sarkar and Phillips (1992a, b). The more general case for arbitrary inclined thermal and solutal gradients was treated by Nield et al. (1993) and independently but in a less detailed manner by Parthiban and Patil (1994). Even when the gradients are coplanar the situation is complex. The effect of the horizontal gradients may be to either increase or decrease the critical vertical Rayleigh number, and the favored mode may be oscillatory or nonoscillatory and have various inclinations to the plane of the applied gradients according to the signs of the gradients. The horizontal gradients can cause instability even in the absence of any vertical gradients. The non-coplanar case was also treated by Nield et al. (1993). A nonlinear stability analysis was presented by Guo and Kaloni (1995a). Their main theorem was proved for the coplanar case. Kaloni and Qiao (2000) extended this analysis to the case of horizontal mass flow. A linear instability analysis for the extension where there is net horizontal mass flow was reported by Manole et al. (1994).

The case of horizontal temperature and vertical solutal gradients was investigated numerically by Mohamad and Bennacer (2001, 2002) and both analytically and numerically by Kalla et al. (2001b). Bennacer et al. (2004, 2005) analyzed convection in a two-layer medium with the lower one thermally anisotropic and submitted to a uniform horizontal heat flux and a vertical mass flux.

Mansour et al. (2004, 2006) studied numerically the Soret effect on multiple solutions in a square cavity with a vertical temperature gradient and a horizontal concentration gradient. Bourich et al. (2004a) showed that the multiplicity of solutions is eliminated if the buoyancy ratio N exceeds some critical value that depends on Le and Ra. A similar problem with a partly heated lower wall was treated by Bourich et al. (2004b). A vertical slot heated from below and with horizontal concentration gradients was studied analytically and numerically by Bahloul et al. (2004a). Convection in a shallow cavity was treated by Bahloul et al. (2007). Further work with a shallow layer was performed by Mansour et al. (2007a, b, 2008a, b) and Narayana et al. (2008). A numeral study of an anisotropic porous medium was conducted by Oueslati et al. (2006). Absolute/convective stability for the case of Soret-driven convection with inclined thermal and solutal gradients was studied by Brevdo and Cirpka (2012).

9.6 Mixed Double-Diffusive Convection

9.6.1 Mixed External Convection

9.6.1.1 Vertical Plate

Similarity solutions also can be obtained for the double-diffusive case of Darcy mixed convection from a vertical plate maintained at constant temperature and concentration (Lai 1991a). The relative importance of buoyancy and forcing effects is critically dependent on the values of Le and *N*. Another study of mixed convection was made by Yücel (1993). Studies with variable wall temperature and concentration were made by Yih (1998f). Mixed convection over a vertical plate with viscosity variation was analyzed by Chamkha and Khanafer (1999). The case of variable heat and mass flux was studied by Singh (2010).

Darcy-Forchheimer convection over a vertical plate was investigated by Jumar et al. (2001), and a similar problem with double dispersion was analyzed by Murthy (2000). For thermally assisted flow, suction increases the local surface heat and mass transfer rates. The case of transverse spatially periodic suction that produces a three-dimensional flow was analyzed by Sharma (2005).

The effect of radiation was considered by Murthy et al. (2005) and Salem (2006a) (viscous dissipation). The effects of viscous dissipation, quadratic drag, and chemical reaction were considered by Mahdy and Chamkha (2010). Soret and Dufour effects for the case of a temperature-dependent viscosity were studied by El-Kabeir (2012). The effect of cross-diffusion was also treated by Sallam (2010), Shateyi and Motsa (2012a) (chemical reaction), and Srinivasacharya and Surenda (2014c) (double stratification). Other studies were made by Afifi and Elgazery (2013) (double dispersion), Khan and Pop (2013) (triple diffusion), Srinivasacharya and Surenda (2014c) (double stratification), Hemalatha et al. (2015) (melting), and Rosca et al. (2015).

A non-Newtonian fluid was studied by Chamkha and Al-Humoud (2007), Chamkha and Ben-Nakhi (2007), Kairi and Murthy (2010) (double dispersion), Mahdy (2010b) (cross-diffusion), Patil et al. (2012) (polar fluid, chemical reaction, internal heating), Srinivasacharya and Swamy Reddy (2012a, b, c, 2013b) (cross-diffusion, radiation, chemical reaction), Srinivasacharya and Ramreddy (2012, 2013b) (micropolar fluid, double stratification, chemical reaction, radiation), Srinivasacharya and Kaladhar (2012, 2014) (couple-stress fluid, cross-diffusion), Mahmoud and Megahed (2013) (cross-diffusion, radiation), and Patil and Chamkha (2012) (polar fluid, chemical reaction).

The effect of a magnetic field was included by Chamkha and Khaled (1999, 2000a, b), Chamkha (2000), Hsiao (2009) (viscoelastic fluid, stretching sheet), Pal and Talukdar (2010) (chemical reaction), Abdel-Rahman (2008) (heat generation), Chamkha and Ben-Nakhi (2008) (cross-diffusion), Shateyi et al. (2010) (cross-diffusion), Mandy (2010) (non-Newtonian fluid), Kandasamy and Muhaimin (2010a) (variable viscosity, thermophoresis, stretching sheet), Makinde (2011b), Srinivasacharya and RamReddy (2011b), Pal and Mondal (2010a, b, 2012a, b, d, 2013) (chemical reaction, cross-diffusion, stretching sheet, nonuniform source, variable viscosity, heat generation, partial slip), Pal and Chatterjee (2011) (micropolar fluid, cross-diffusion, stretching sheet), Shateyi and Motsa (2011) (radiation, stretching sheet), Jaber (2011) (transient flow, suction/injection), Mondal and Mukhopadhyay (2012) (stretching sheet), Aurangzaib et al. (2013a, b) (unsteady stagnation point flow, micropolar fluid, cross-diffusion), Pal and Chatterjee (2014) (viscoelastic fluid, stretching sheet, chemical reaction), Nayak et al. (2014b) (cross-diffusion, stretching sheet, chemical reaction), Najafabadi and Gorla (2014) (stretching sheet), Khidir and Sibanda (2014a) (stretching sheet, cross-diffusion, temperature-dependent viscosity), Hussanan et al. (2015) (cross-diffusion, unsteady flow, Newtonian heating), Waheed et al. (2015) (micropolar fluid, cross-diffusion, chemical reaction, radiation, slip), Kishan and Jaghadha (2016), (thermophoresis, radiation), and Karthikeyan et al. (2016) (stagnation point flow, cross-diffusion, chemical reaction, radiation, heat generation).

Convection over a vertical stretching surface was also studied by Hayat et al. (2010a) (viscoelastic fluid, cross-diffusion), Tsai and Huang (2009b) (Hiemenz flow, cross-diffusion), Rashad and El-Khabeir (2010) (unsteady flow), Pal and Mondal (2012c) (cross-diffusion, chemical reaction, radiation), and Srinivasacharya and Ramreddy (2013a) (cross-diffusion).

9.6.1.2 Other Surfaces

A wavy vertical surface with cross-diffusion and variable properties was studied by Srinivasachrya et al. (2015a).

Mixed convection in an inclined layer was analyzed by Rudraiah et al. (1987). The influence of lateral mass flux on mixed convection over inclined surfaces was analyzed by Singh et al. (2002) and Bansod et al. (2005).

Kumari and Nath (1992) studied convection over a slender vertical cylinder, with the effect of a magnetic field included. The effect of transpiration on mixed convection past a vertical permeable plate or vertical cylinder was treated numerically by Yih (1997a, b, 1999h). For convection about a vertical cylinder, the entire mixed convection regime was covered by Yih (1998g, 1999j) and Chamkha et al. (2011c) studied the case of temperature-dependent viscosity.

Mixed convection over a wedge or a cone with variable wall temperature and concentration was analyzed by Yih (1998c, f, 1999b, c, 2000b). A cone was also studied by Mallinkarjuna et al. (2016) (magnetic field, rotation, chemical reaction).

A wedge was also studied by Hassanien et al. (2003a) (uniform heat and mass flux), Seddeek et al. (2007) (magnetic field, radiation, chemical reaction, variable viscosity), Muhaimin et al. (2009a, b, 2010a) (magnetic field, chemical reaction, variable viscosity, thermophoresis), Kandasamy and Muhaimin (2010b) (magnetic field, suction, thermophoretic particle deposition), Kandaswamy et al. (2007, 2008d) (suction/injection, variable viscosity), Kandasamy et al. (2010b) (variable viscosity, thermophoresis), and Cheng (2012b, g) (cross-diffusion).

Mixed convection about a sphere with a chemical reaction was studied by Rashad et al. (2011b).

9.6.2 Mixed Internal Convection

A numerical study of mixed convection with opposing flow in a rectangular cavity with horizontal temperature and concentration gradients was reported by Younsi et al. (2002a, b), who noted that for a certain combination of Ra, Le, and N values the flow has a multicellular structure. Mixed convection driven by a moving lid of a square enclosure was studied numerically by Khanafer and Vafai (2002) for the case of insulated vertical walls and horizontal at different constant temperature and concentration. Convection in a vertical wavy channel with traveling thermal waves was examined by Muthuraj and Srinivas (2010). A nonuniformly heated vertical channel with heat sources and dissipation was studied numerically by Nath et al. (2010). Couette flow of an MHD viscoelastic fluid was treated by Eldabe and Sallam (2005). Srinivas and Muthuraj (2011) studied the effects of MHD, chemical reaction, peristalsis, and the special variation of porosity for flow in a vertical channel with asymmetric boundary conditions. Forced convection, but with coupled heat and mass transfer, in a channel with chemical reaction was investigated by Bousri et al. (2011) and Li et al. (2013b) (local thermal nonequilibrium). Convection in a vertical pipe with local thermal nonequilibrium was studied by Bera et al. (2012a, b). A vertical pipe was also studied by Kapoor et al. (2012). A box with stratification and injection/suction was studied by Rathish Kumar and Krishna Murthy (2012b). A vertical pipe with cross-diffusion in a vertical channel was treated by Alloui and Vasseur (2013b). Convection in a lid-driven box was studied by Misra et al. (2013). Unsteady flow in a vertical corrugated composite channel was studied by Umavathi and Shekar (2013). Pulsatile flow in an inclined porous channel with

chemical reaction was analyzed by Srinivas et al. (2014). The combination of cross-diffusion and endothermic reaction was studied by Li et al. (2013a, b). A two-sided lid-driven cavity was examined by Agarwal et al. (2015). Dey and Sekhar (2014) studied mass transfer and species separation due to oscillatory flow in a pipe. Unsteady MHD oscillatory flow of a Casson fluid in a wavy channel was investigated by Sivaraj and Benazir (2016). A numerical simulation of MHD flow in a lid-driven cavity was made by Mohan and Satheesh (2016). MHD flow in a vertical channel with cross-diffusion was studied by Reddy et al. (2016a). Li et al. (2013a, b) examined forced convection with cross-diffusion, local thermal nonequilibrium, and endothermic reactions. Bousri et al. (2017) investigated numerically forced convection with local thermal nonequilibrium. Ghalambaz et al. (2017) studied mixed convection with triple diffusion in an open cavity.

9.7 Nanofluids

The reader is referred to Sect. 3.8 for an introduction to nanofluids.

Convection in porous media saturated by nanofluids has been reviewed by Barletta et al. (2015b), Mahdi et al. (2015a), Nield and Kuznetsov (2015a, b) and Kasaeian et al. (2017).

9.7.1 Forced Convection

Thermally developing forced convection of a nanofluid in a parallel-plate channel was studied numerically by Maghrebi et al. (2012), who employed the Buongiorno model with thermophoresis and Brownian motion. They found that the local Nusselt number is decreased when the Lewis number Le is increased and when the Schmidt Sc number is increased, these parameters being defined by

$$\mathrm{Le} = \frac{\alpha_\mathrm{m}}{\phi_0 D_\mathrm{B}}, \quad \mathrm{Sc} = \frac{\mu}{\rho D_\mathrm{B}}, \tag{9.64}$$

where α_m is the effective thermal diffusivity, D_B is the Brownian diffusion coefficient, ϕ_0 is the particle fraction at the channel inlet, μ is the nanofluid viscosity, and ρ is the nanofluid density. Armaghani et al. (2014b) extended this study to include the effect of local thermal nonequilibrium (LTNE). Further numerical work with LTNE, first taking into account of particle migration and then using a model in which the heat flux in each of the phases is considered, was carried out by Armaghani et al. (2014a, b). LTNE in a microchannel with viscous dissipation was studied by Ting et al. (2014, 2015a).

On the other hand, in his analytical study of flow in microchannels, Hung (2010) considered just the variation of thermal conductivity, viscosity, and heat capacity.

A more general analytical study using the Buongiorno model was made by Nield and Kuznetsov (2014b). They examined flow in a Darcy porous medium occupying a parallel-plane channel with uniform heat flux on the boundaries. They found that the combined effect of Brownian motion and thermophoresis is to reduce the Nusselt number. The reduction increases as $N_A N_B/\varepsilon$ increases, where N_A and N_B are defined by

$$N_A = \frac{D_T}{D_B T^*_w}, \quad N_B = \frac{\varepsilon(\rho c)_p \phi^*_0}{(\rho c)_f}, \tag{9.65}$$

and so

$$\frac{N_A N_B}{\varepsilon} = \frac{D_T}{D_B} \frac{(\rho c)_p \phi^*_0}{(\rho c)_f T^*_w}, \tag{9.66}$$

that is the product of a diffusivity ratio and a heat capacity ratio. Nield and Kuznetsov (2014b) noted that this reduction in heat transfer due to a modification of the temperature profile by Brownian motion and thermophoresis would oppose any increase due to the thermal conductivity of the nanofluid being higher than that of a regular fluid. This result applies only to the case where the Péclet number based on the thermophoresis diffusivity is small compared with unity. It was pointed out by Nield and Kuznetsov (2014c) that net throughflow produces an extra contribution to the nanoparticle flux and hence an additional term into the thermal energy equation.

A nanofluid with property variation has been studied by several authors. Matin and Pop (2013) studied heat and mass transfer with a chemical reaction on the walls. Nasrin and Alim (2013) and Nasrin et al. (2013a, b) have considered a problem with an open cavity. Baqaie Saryazdi et al. (2016) studied numerically flow in a pipe. Dickson et al. (2016) reported first and second law analyses of flow in a partly filled pipe with the effects of local thermal nonequilibrium and internal heat sources. The effect of a magnetic field has been studied by Servati et al. (2014), Sulochansa and Sandeep (2015) (radiation, slendering stretching sheet), Ibanez et al. (2016) (microchannel, slip, entropy generation, radiation), and Moshizi (2015) (microchannel, chemical reaction on the walls). Forced convection of a non-Newtonian fluid in an annulus was examined by Ellahi et al. (2013). Hatami et al. (2014) studied an asymmetric porous channel with expanding or contracting wall. A channel with discrete heat sources was investigated by Mashaei and Hossainalipour (2014). An experimental study with a pipe filled with metallic foam was reported by Nazari et al. (2014a, b). An analytical study, involving volume averaging, for convection in metallic foams, was reported by Zhang et al. (2015b). A numerical study of metallic foams was made by Xu et al. (2015b). Ting et al. (2015b, c) studied viscous dissipative convection in asymmetrically heated microchannels with solid-phase heat generation. Torabi et al. (2016a) investigated entropy generation in a partly filled channel with thermal nonequilibrium. Nazari

et al. (2014a) reported an experimental study for flow through a pipe filled with metallic foam. Mashaei et al. (2016b) studied convection in a narrow annulus. Nojoomizadeh and Karimpour (2016) studied the effects of porosity and permeability on convection in a microchannel with multi-walled carbon nanotubes suspended in oil. Bayomy and Saghir (2017) experimented with the flow of a nanofluid through an aluminium foam heat sink. Nazari and Toghraie (2017) numerically simulated convection of a water-CuO nanofluid in a sinusoidal channel.

9.7.2 Internal Natural Convection

9.7.2.1 Horizontal Layer

The Horton-Rogers-Lapwood problem was treated using the Buongiorno model by Nield and Kuznetsov (2009b), Kuznetsov and Nield (2010a, 2011a, b, c) (local thermal nonequilibrium), Kuznetsov and Nield (2010b) (Brinkman model), Kuznetsov and Nield (2010c) (double diffusion), Nield and Kuznetsov (2011d) (vertical throughflow) (corrected by Jaimala and Singh, 2014), Sheu (2011) (viscoelastic fluid), Bhadauria and Agarwal (2011a, b), Agarwal and Bhadauria (2011), and Bhadauria et al. (2011a, b) (nonlinear instability, rotation, local thermal nonequilibrium), Agarwal et al. (2011) (rotation, anisotropy), Agarwal et al. (2012) (nonlinear transport), Agarwal (2014) (rotation with a revised model), Agarwal and Rana (2015a) (rotation, local thermal nonequilibrium), Agarwal and Rana (2015b, 2016) (binary nanofluid with cross-diffusion, rotation), and Yadav et al. (2016a, b, d) (dielectic nanofluid, magnetic field, quadratic drag), Chand et al. (2016) (electroconvection) and Rana et al. (2016) (Rivlin-Eriksen fluid). In these papers the significant effects were those of Brownian motion and thermophoresis. An alternative model, incorporating the effects of conductivity and viscosity variation and with cross-diffusion also included, was examined by Nield and Kuznetsov (2012a, b). The effect of rotation was also studied by Chand and Rana (2012d). Bioconvection in nanofluids with either gyrotactic or oxytactic microorganisms or both was investigated by Kuznetsov (2012a, b) and Kuznetsov and Bubnovich (2012), and also by Shaw et al. (2014a, b). Boundary and internal source effects were treated by Yadav et al. (2012). The problem of double diffusion combined with variation of thermal conductivity and viscosity was examined by Yadav et al. (2013a, b). The singular case of a non-Newtonian power-law fluid was discussed by Nield (2011a, b). The above studies involved bottom heating. The case of uniform volumetric heating was investigated by Nield and Kuznetsov (2013b). In this paper, zero particle-flux boundary conditions were employed. The Horton-Rogers-Lapwood problem was revisited by Nield and Kuznetsov (2014c). This time they treated the more realistic case of zero particle-flux boundary conditions. They showed that in this case oscillatory instability was ruled out. They obtained an approximate expression for the nonoscillatory instability boundary in the form

$$\mathrm{Ra} = 40 - \left(N_\mathrm{A} + \frac{\mathrm{Le}}{\varepsilon}\right)\mathrm{Rn}, \tag{9.67}$$

this boundary being attained with a dimensionless wavenumber $\alpha = 3.16$. Here ε is the porosity, Ra is the usual Rayleigh-Darcy number, Rn is a nanofluid Rayleigh number, Le is a Lewis number, and N_A is a modified diffusivity ratio now defined by

$$\mathrm{Ra} = \frac{\rho g \beta K H \left(T_\mathrm{h}^* - T_\mathrm{c}^*\right)}{\mu \alpha_\mathrm{m}}, \tag{9.68}$$

$$\mathrm{Rn} = \frac{\left(\rho_\mathrm{p} - \rho\right)\phi_0^* g K H}{\mu \alpha_\mathrm{m}}, \tag{9.69}$$

$$\mathrm{Le} = \frac{\alpha_\mathrm{m}}{D_\mathrm{B}}, \tag{9.70}$$

$$N_\mathrm{A} = \frac{D_\mathrm{T}\left(T_\mathrm{h}^* - T_\mathrm{c}^*\right)}{D_\mathrm{B} T_\mathrm{c}^* \phi_0^*}, \tag{9.71}$$

where T_h^* and T_c^* are the temperature at the bottom and top boundaries and ϕ_0^* is a reference nanoparticle volume fraction. The case of vertical throughflow was studied using the revised model by Nield and Kuznetsov (2015b). A layer with internal heating was examined by Nield and Kuznetsov (2013c).

Other studies were made by Shivakumara et al. (2010a, b, c, d) (magnetic fluid), Bhadauria et al. (2011a) (nonlinear convection), Chand and Rana (2012a) (oscillatory convection), Chand and Rana (2012c) (viscoelastic fluid), Shaw and Sibanda (2013) (vertical throughflow, convective boundary condition), Umavathi (2013b) (thermal modulation), Yadav et al. (2013a) (double diffusion, variable viscosity and conductivity), Bhadauria and Kiran (2014a) (gravity modulation), Chand and Rana (2014), Kang et al. (2014a) (heterogeneous power-law fluid, horizontal throughflow), Mahajan and Sharma (2014) (magnetic nanofluid), Rana et al. (2014a) (double diffusion, rotation), Rana et al. (2014b) (double diffusion, viscoelastic fluid), Umavathi and Mohite (2014a, b) (cross-diffusion, variable viscosity and conductivity), Sharma and Singh (double diffusion, magnetic nanofluid), Yadav and Kim (2014a) (cross-diffusion, rotation, transient convection), Yadav et al. (2014) (rotation, non-Newtonian fluid, variable viscosity and conductivity), Chand et al. (2015a) (low Prandtl number fluid), Chand et al. (2015b) (rotation, variable gravity), Rana and Chand (2015) (double diffusion, viscoelastic fluid), Shivakumara et al. (2015a) (viscoelastic fluid), Shivakumara and Dhananjaya (2015) (penetrative convection, anisotropy), Umavathi (2015b) (time-dependent wall temperature), Umavathi et al. (2015a, b) (nonlinear stability, double diffusion, viscoelastic fluid, variable viscosity and conductivity, cross-diffusion), Yadav and Kim (2015a) (transient flow, double diffusion, concentration-dependent viscosity), Yadav et al. (2015) (internal heating, rotation), Chand et al. (2016) (electro-thermal convection), Ahuja et al. (2016) (magnetic field), Sharma et al. (2016a, b)

(magnetic field, double diffusion), and Umavathi and Prathap Kumar (2017) (Oldroyd-B fluid) Kiran (2014) (viscoelastic fluid, gravity modulation).

The onset of Soret-driven convection in a Hele-Shaw cell or porous medium was studied by Kim (2014c).

9.7.2.2 Rectangular Box

A rectangular cavity was studied by Sheikhzadeh and Nazari (2013) (square), Bourantas et al. (2014) (square cavity, sidewall heating), Sheremet and Pop (2014a) (conjugate problem, Buongiorno model), Sheremet and Pop (2014b) (sinusoidal distributions on both sidewalls, Buongiorno model), Sheremet et al. (2014) (shallow and slender cavities, Buongiorno model), Sheremet et al. (2015b) (square), Sheremet et al. (2015b) (square), Grosan et al. (2015) (square, Buongiorno model), Sheremet et al. (2015a) (square, thermal stratification), Sheremet et al. (2015d) (square, Buongiorno model, 3D convection), Sheremet et al. (2015f) (local thermal nonequilibrium), Sheremet et al. (2015c) (cubical cavity, Tiwari and Das model), Hossain et al. (2015) (transient, phase change material), Nguyen et al. (2015), Shekar and Kishan (2016) (radiation), Kefayati (2016c) (power-law fluid, sidewall heating), Satheesh and Raj (2016) (sidewall heating, moving sidewalls), Ismael et al. (2016) (conjugate heat transfer, entropy generation, heated by a triangular solid), Pop et al. (2016) (square, sidewall heating, local thermal nonequilibrium, Buongiorno model), Rashad et al. (2017) (magnetic field, internal heat generation), Ahmed and Rashad (2016) (micropolar fluid, anisotropy), Muthtamilselvan and Sureshkumar (2016) and Ashorynejad and Mosseinpour (2017) (entropy generation).

A square cavity heated along a segment of the bottom wall was studied by Bourantas et al. (2014) .

9.7.2.3 Vertical or Inclined Channel, Vertical Pipe

The case of a vertical channel was studied by Hajipour and Dehkordi (2012a, b) (partly filled channel), Akbar (2014) (double diffusion, Jeffrey fluid, peristaltic flow), Chamkha and Ismael (2014) (partly filled, differentially heated), Das et al. (2015b) (MHD, pseudoplastic fluid, entropy analysis, convective heating), Akbar (2015) (double diffusion, peristaltic flow, asymmetric channel), Govender (2016a) (rotation, Buongiorno model), Govender (2016b) (rotation about an axis at a finite distance) and Umavathi et al. (2017) (Forchheimer-Brinkman model) and Raza et al. (magnetic field, stretching walls, semi-porous channel. Al-Zamily (2017) studied entropy generation in a vertical channel with a porous core and a heat-generating nanofluid. Lopez et al. (2017) analyzed entropy generation in a vertical microchannel with a magnetic field, nonlinear thermal radiation, slip flow and a convective-radiative boundary condition.

An inclined channel was examined by Shaw et al. (2014b) (magnetic field, cross-diffusion, bioconvection) and Bondareva et al. (2016) (wavy channel, magnetic field, local heater), and Umavathi et al. (2017) (Forchheimer-Brinkman model) and Raza et al. (magnetic field, stretching walls, semi-porous channel. Al-Zamily (2017) studied entropy generation in a vertical channel with a porous core and a heat-generating nanofluid. Lopez et al. (2017) analyzed entropy generation in a vertical microchannel with a magnetic field, nonlinear thermal radiation, slip flow and a convective-radiative boundary condition. Transient convection in an oblique cavity was studied by Alsabery et al. (2016a) using a thermal nonequilibrium model. An inclined square enclosure was studied by Yekani Motlagh et al. (2016) using the Buongiorno model.

Unsteady convection in a vertical pipe with slip was studied by Khamis et al. (2015).

9.7.2.4 Other Cavities

Double diffusive convection with thermo-diffusion in a square cavity subject to various heating conditions was studied numerically by Ahadi et al. (2013). A triangular cavity with a flush mounted heater on a wall was treated numerically by Sun and Pop (2011, 2014) and Ahmed et al. (2013a, b). A triangular cavity was also studied by Sheremet and Pop (2015d) (Buongiorno model). A trapezoidal cavity was studied by Alsabery et al. (2015) (heatline visualization, partly filled and partly non-Newtonian fluid) and Sheremet et al. (2015d) (Buongiorno model, right-angled). An inclined trapezoidal cavity was studied by Ahmed (2014a, b). Conjugate problems, with a cavity heated by a plane or triangular thick wall, were investigated by Chamkha and Ismael (2013b). Convection in an H-shaped enclosure with mounted heaters on the vertical walls was examined by Mansour et al. (2014). A cavity with wavy top and bottom and with sinusoidal distributions on both sidewalls was studied by Sheremet and Pop (2015a, 2016), with the Buongiorno model in the second paper. A horizontal annulus was treated by Sheremet and Pop (2015b, c) (Buongiorno model). A parallelogrammic cavity was treated by Ghalambaz et al. (2015a, b). Unsteady convection in an open cavity was studied by Sheremet et al. (2015g) (Buongiorno model). Transient convection in a wavy-walled cavity was investigated by Sheremet et al. (2016a), while Sheremet et al. (2016b) examined MHD convection, in a wavy open tall cavity, produced by a corner heater. The effect of radiation and magnetic field on peristaltic transport in a tapered porous channel was studied by Kothandapani and Prakash (2015). An inclined square cavity with a magnetic field was treated by Balla et al. (2016). An inclined square cavity with a centrally placed fluid-filled square hole was studied by Alsabery et al. (2016b). A wavy open cavity was investigated by Sheremet et al. (2016a, b, c). A triangular cavity was treated by Sabour and Ghalambaz (2016) using the Buongiorno model and three heat equations. The Buongiorno model was also used by Zargartalebi et al. (2016) in their study of an enclosure containing an inclined porous fin. Double diffusion in a triangular

enclosure with heat generation was studied by Chowdhury et al. (2016). A partly open cavity with internal heating was treated by Nithyadevi and Rajarathinam (2016a, b). A magnetic nanofluid was examined by Sheikholeslami (2016) (curved enclosure) and Sheikholeslami and Shezad (2017) (heat flux boundary condition). The effects of finite wall thickness, sinusoidal heating and local thermal non-equilibrium on convection in a cavity were studied by Alsabery et al. (2017). Buongiorno's model was applied to a porous wavy cavity with a thermal dispersion effect by Sheremet et al. (2017).

9.7.3 External Natural Convection

9.7.3.1 Vertical Plate

The Cheng-Minkowycz problem of boundary layer flow over a vertical plate at constant temperature was studied by Nield and Kuznetsov (2009a, 2011a) and (with a revised model, employing zero particle-flux boundary conditions) by Kuznetsov and Nield (2013a, b), who obtained a linear regression correlation formula for a Nusselt number of the form

$$\mathrm{Nu_{est}}/\mathrm{Ra_x}^{1/2} = 0.444 + C_\mathrm{r}\mathrm{Nr} + C_\mathrm{b}\mathrm{Nb} + C_\mathrm{t}\mathrm{Nt}, \tag{9.72}$$

where the coefficients are functions of Le/ε, given by Table 9.3. Here Le is the Lewis number defined by Eq. (9.69) and the local Rayleigh number Ra and the parameters Nr, Nb, and Nt are defined by

$$\mathrm{Ra}_x = \frac{(1-\phi_\infty)\rho_{f\infty}\beta g K x}{\mu\alpha_\mathrm{m}}, \tag{9.73}$$

$$\mathrm{Nr} = \frac{(\rho_p - \rho_{\mathrm{f}\infty})\phi_\infty}{\rho_{\mathrm{f}\infty}\beta(T_\mathrm{w} - T_\infty)(1-\phi_\infty)}, \tag{9.74}$$

Table 9.3 Summary of linear regression coefficients and error bound for the reduced Nusselt number, applicable to Eq. (9.71)

Le/ε	C_r	C_b	C_t	ε
5	−0.003	0.004	−0.090	0.030
10	−0.001	0.000	−0.105	0.009
20	−0.001	−0.001	−0.120	0.003
50	−0.002	−0.002	−0.135	0.004
100	−0.002	−0.003	−0.143	0.005
200	−0.003	−0.003	−0.150	0.006
500	−0.003	−0.003	−0.155	0.006
1000	−0.003	−0.003	−0.158	0.007

Here ε is the maximum relative error defined by $\varepsilon = |(\mathrm{Nu_{est}} - \mathrm{Nu})/\mathrm{Nu}|$, applicable for Nr, Nb, Nt each in [0, 0.5]

$$\mathrm{Nb} = \frac{\varepsilon(\rho c)_{\mathrm{p}} D_{\mathrm{B}} \phi_{\infty}}{(\rho c)_{\mathrm{f}} \alpha_{\mathrm{m}}}, \tag{9.75}$$

$$\mathrm{Nt} = \frac{\varepsilon(\rho c)_{\mathrm{p}} D_{\mathrm{T}} (T_{\mathrm{w}} - T_{\infty})}{(\rho c)_{\mathrm{f}} \alpha_{\mathrm{m}} T_{\infty}}. \tag{9.76}$$

It can be seen in the table that the Brownian motion parameter Nb has very little effect on the Nusselt number and the coefficient of the buoyancy ratio Nr is also small. The Nusselt number is reduced as the thermophoresis parameter Nt is increased.

Other studies of a vertical plate were reported by Gorla and Chamkha (2011a) (nonisothermal plate), Hady et al. (2011b, c) (non-Newtonian fluid, yield stress), Noghrehabadi et al. (2013c) (prescribed surface heat flux), Ghalambaz and Noghrehabadi (2014) (prescribed surface heat flux), Tavakoli et al. (2013) (non-Darcy medium), Aziz et al. (2012) (bioconvection), Khan et al. (2013a) (non-Newtonian fluid, bioconvection), Uddin et al. (2013a, b) (non-Newtonian fluid, bioconvection), RamReddy et al. (2014) (stratification), Srinivasacharya and Surenda (2014d) (double stratification), Noghrehabadi et al. (2014a, b) (variable viscosity and conductivity), Murthy et al. (2013a) (magnetic field, thermal stratification, convective boundary condition), Uddin et al. (2013c) (non-Newtonian fluid, internal heating), Uddin and Harmand (2013) (unsteady flow), RamReddy and Chamkha (2013) (non-Newtonian fluid), Satya Narayana et al. (2014) (rotation, radiation), RamReddy et al. (2013b) (magnetic field), Kameswaran and Sibanda (2013) (power-law fluid, thermal dispersion), Noghrehabadi et al. (2014a, b), Chamkha et al. (2014c) (internal heating), Chamkha et al. (2014d) (magnetic field), Ali Agha et al. (2014) (magnetic field, radiation), Chandra et al. (2014a) (suction/injection, internal heating), Chandra et al. (2014b) (viscous dissipation, convective boundary condition), (Dehsara et al. (2014) (magnetic field, radiation), Ghalambaz et al. (2014) (convectively heated plate), Mabood et al. (2014) (non-Newtonian fluid, bioconvection), Muthtamilselvan et al. (2014a, b) (transient convection, magnetic field, local thermal nonequilibrium), Surenda (2014) (double stratification), Srinivasacharya and Surenda (2014d) (cross-diffusion, double stratification), Uddin et al. (2014a) (double diffusion, radiation, magnetic field, slip flow), Awad et al. (2015) (double dispersion), Khan et al. (2015a, b, d, e) (triple diffusion), Zhang et al. (2015a, b, c) (magnetic field, chemical reaction, radiation), Abou-zeid et al. (2015) (power-law nanoslime), Agha et al. (2014, 2015) (magnetic field, radiation), (magnetic field, multiple slip effects, unsteady flow, heat generation, temperature-dependent properties), Hayat et al. (2015a) (magnetic field, convective boundary conditions), Khan et al. (2015a, b) (non-Newtonian fluid, bioconvection, slip), Rashidi et al. (2015b) (entropy generation), Uddin et al. (2015b) (magnetic field), Narayana et al. (2015) (magnetic field, rotation, heat source), Uddin et al. (2016a, b, d) (Buongiorno model, radiation, non-Newtonian fluid, magnetic field, stretching sheet), Ahmed and Mahdy (microorganisms, magnetic field, Buongiorno model), Bouaziz and Hanini (2016) (double dispersion), Kiran Kumar et al. (2016) (rotation, magnetic

field, chemical reaction), Aly and Ebaid (2016) (magnetic field, surface tension, radiation), Mohd Zin et al. (2016) (magnetic field, Jeffrey fluid, oscillating plate), Haile and Shankar (2016) (magnetic field, radiation), and Kataria and Mittal (2017) (oscillating plate, magnetic field).

A stretching surface was treated by Ferdows et al. (2012) (magnetic field), Khan and Pop (2012b), Rosmila et al. (2012), Sheikholeslami and Ganji (2014), Sheikholeslami et al. (2014), Aly and Hassan (2014) (magnetic field), Khidir and Sibanda (2014b) (viscous dissipation), Hayat et al. (2014) (convective boundary condition, exponential stretching), Khalili et al. (2014a), Kameswaran et al. (2014a) (internal heating),Uddin et al. (2014b) (g-jitter, slip flow, variable viscosity), Hayat et al. (2015b) (magnetic field, chemical reaction), Yirga and Shankar (2015) (magnetic field, viscous dissipation, chemical reaction), Uddin et al. (2015a) (Newtonian heating, radiation, Buongiorno model), Khan et al. (2016a, b) (cross-diffusion), Reddy and Chamkha (2016) (cross-diffusion, heat generation), Sulochana et al. (2016) (aligned magnetic field, cross-diffusion, exponential stretching), Aly (2016b) (magnetic field, radiation) and Ullah et al. (2016b) (magnetic field, Casson fluid, radiation, chemical reaction) and Vishnu Ganesh et al. (2016) (magnetic field, second order slip, viscous dissipation).

Stagnation point flow on a heated permeable stretching surface with heat generation/absorption was studied by Hamad and Pop (2011). This paper was discussed by Magyari (2011a, b) and Pop (2011). Stagnation point flow was also studied by Khan and Pop (2012a, b), Khalili et al. (2014a, b) (magnetic field, stretching surface, unsteady flow), Yazdi et al. (2014) (magnetic field, radiation, stretching surface), Pal et al. (2014) (stretching surface), Mabood et al. (2016b) (magnetic field, radiation, chemical reaction, viscous dissipation), and Shaw et al. (2016) (stretching sheet, dual solutions, chemical reaction).

Flow over a wavy vertical wall was studied by Mahdy and Ahmed (2012) and Ahmed and Abd El-Aziz (2013) (local thermal nonequilibrium, unsteady convection).

9.7.3.2 Horizontal or Inclined Plate or Wedge

The case of a heated upward facing horizontal flat plate was considered by Khan and Pop (2011a), Gorla and Chamkha (2011b, c), Uddin et al. (2012a, b), Uddin et al. (2013a, b, c) (power-law fluid, internal heating, bioconvection), Khan et al. (2013c) (triple diffusion), Rashidi et al. (2014a) (chemical reaction), Zargartalebi et al. (2015) (variable thermo-physical properties), and Uddin et al. (2016a) (slip).

An inclined plate was investigated by Cheng (2012e) (cross-diffusion), Murthy et al. (2013b) (double diffusion), Srinivasacharya and Vijay Kumar (2015a) (wavy surface, radiation), and Srinivasacharya et al. (2016).

An isothermal wedge with cross-diffusion was studied by Kameswaran et al. (2014c). Flow over a wedge was also studied by Chamkha et al. (2011c) and Kandasamy et al. (2012, 2013, 2014). Kandasamy et al. (2016) added the effects

of a magnetic field and thermal radiation energy. A wedge with magnetic field, suction/injection and viscous dissipation was studied by Pandey and Kumar (2016).

9.7.3.3 Curved Surface

Flow over a vertical cylinder was treated by El-Kabeir et al. (2014). A vertical cylinder embedded in a thermally stratified porous medium was studied by Rashad et al. (2014c).

Flow over a horizontal cylinder of elliptical cross section was investigated by Cheng (2012a). A stretching horizontal cylinder with radiation and suction/injection was studied by Elbashbeshy et al. (2015). Convection from a horizontal cylinder in a square enclosure was treated by Saleh and Hashim (2015). A horizontal cylinder with double diffusion was studied by Sudarsana Reddy and Chamkha (2016b) using the Buongiorno model.

Convection over a vertical cone was examined by Rashad et al. (2011c), Cheng (2012c), Chamkha and Rashad (2012), Hady et al. (2011a) (non-Newtonian fluid), Rasekh et al. (2013) (non-Newtonian fluid), Noghrehabadi et al. (2013b), Cheng (2013a) (double diffusion), Behseresht et al. (2014) (double diffusion), Gorla et al. (2014), Cheng (2014c), Ghalambaz et al. (2015a, b) (variable conductivity), Khan et al. (2015d), (power-law fluid, convective boundary conditions), Chamkha et al. (2013b, 2015a) (permeable cone), Sudarsana Reddy and Chamkha (2016), Mahdy et al. (2016) (microorganisms), Hady et al. (2016) and Uddin et al. (2016c) (dilatant nanofluid, multiple convective boundary conditions).

The case of a vertical truncated cone was treated by Cheng (2012f) and (with a non-Newtonian fluid) by Cheng et al. (2012d). Convection about a sphere was studied by Chamkha et al. (2011a, d). Hayat et al. (2016a, b) investigated the effect of variable viscosity and a radial magnetic field on peristalsis in a curved channel.

9.7.4 Mixed Convection

9.7.4.1 Vertical Plate

Mixed convection boundary layer flow over a vertical plate was studied by Ahmad and Pop (2010), Syakila and Pop (2010), Rashad et al. (2013a) (non-Newtonian fluid), Yasin et al. (2012) (internal heating, Ferdows et al. (2012) (magnetic field, stretching sheet), Bég et al. (2013a) (oxytactic microorganisms), Rashad et al. (2013a) (non-Newtonian fluid), Yasin et al. (2013a) (thermal stratification), Yasin et al. (2013a, b) (suction/injection), Ramreddy et al. (2013a) (Soret effect, convective boundary condition), Rashad et al. (2014a) (viscous dissipation), Rosca et al. (2014), Srinivasacharya and Surenda (2014a) (double stratification), Rashad et al. (2014b) (viscous dissipation), Pal and Mondal (2014a, 2015) (stagnation point flow, stretching sheet, chemical reaction, radiation, heat generation, and viscous

dissipation),Yazdi et al. (2014) (stagnation point flow, magnetic field, stretching sheet, radiation), Kairi and RamReddy (2015) (melting, power-law fluid), Rashad et al. (2015) (convective boundary conditions, viscous dissipation), Abdullah and Ibrahim (2015) (unsteady stagnation point flow, Buongiorno model), Srinivasacharya et al. (2015e, 2016) (wavy surface, thermophoresis), Ramzan et al. (2016) (viscoelastic fluid, cross-diffusion), Kameswaren et al.(2016) (wavy surface, stratification, nonlinear Boussinesq approximation), and Yasin et al. (2016) (Buongiorno model).

9.7.4.2 Horizontal or Inclined Plate

Flow past a horizontal plate was investigated by Arifin et al. (2012). Mixed convection from a horizontal plate with Forchheimer drag, but considering only the effect of the nanoparticle volume fraction parameter, was investigated by Rosca et al. (2012). Flow over an inclined plate was studied by Rana et al. (2012b), Aly and Ebaid (2013), Rasekh and Ganji (2013), Matin and Hosseini (2014), and Srinivasacharya and Vijay Kumar (2015b, c) (wavy surface).

9.7.4.3 Curved Surfaces

The corresponding flow over a horizontal cylinder was examined by Nazar et al. (2011) and Tham et al. (2013a). A horizontal cylinder with a convective boundary condition was investigated by Rashad et al. (2013b).

The case of a vertical cylinder was treated by Chamkha et al. (2012), Gorla and Abdel-Gaied (2011), Gorla and Khan (2012), Gorla and Hossain (2013), RamReddy et al. (2013a, b) (double diffusion, cross-diffusion), Rohni et al. (2013), Rashad et al. (2014a, b, c) (thermal stratification), and El-Kabeir et al. (2014) (radiation).

Convection over a sphere or a horizontal circular cylinder with a nanofluid containing gyrotactic microorganisms was studied by Tham and Nazar (2012a, b, 2013) and Tham et al. (2013b, c). Flow past a horizontal cylinder was treated using the Buongiorno model by Tham et al. (2104b, 2016). Flow past a sphere was also treated by Tham et al. (2014a) and by El-Kabeir et al. (2015a, b) (radiation, convective boundary condition). Khan et al. (2015c) studied unsteady MHD rear stagnation point slip flow.

Convection past a vertical cone was treated by Hady et al. (2011a) (non-Newtonian fluid, heat generation/absorption), Rashad et al. (2011c) (non-Newtonian fluid), Chamkha and Rashad (2012) (suction/injection), Chamkha et al. (2013a) (radiation), Rasekh et al. (2013) (non-Newtonian fluid), Cheng (2013a) (double diffusion), Noghrehabadi et al. (2013b), Noghrehabadi and Behseresht (2013) (variable properties), Zeeshan et al. (2014) (magnetic field), Behseresht et al. (2014) (double diffusion, variable properties), Ghalambaz et al.

(2015a, b) (variable conductivity), and Chamkha et al. (2015a, b) (non-Newtonian fluid). A truncated cone was studied by Cheng (2012b).

Flow past a wedge was examined by Gorla and Kumari (2011), Gorla et al. (2011b), Chamkha et al. (2014b), and Kandasamy et al. (2014) (magnetic field, unsteady convection). Shafie et al. (2016), and Aman et al. (2016) (Poiseuille flow, magnetic field, radiation, chemical reaction).

9.7.4.4 Vertical, Horizontal, or Inclined Channel

Mixed convection in a vertical channel was studied by Memari et al. (2011a, b) (viscous heating), Hashemi Amrei and Dehkordi (2014), Matin and Ghanbari (2014) (Buongiorno model, flow reversal), Hashemi Amrei and Dehkordi (2014) (partly filled channel), Hajipour and Dehkordi (2014) (experimental study with partly filled channel) Sheremet et al. (2015a, b, c, d, e, f, g, h) (double diffusion, open cavity, Buongiorno model), Fersdaou et al. (2015)(MHD, entropy generation), Makhata et al. (2015) (flow reversal, variable viscosity, convective surface condition), Sarkar et al. (2015) (wavy channel, peristaltic flow, radiation), Aaiza et al. (2015) (magnetic field), and Rauf et al. (2016) (stretchable channel, radiation, microfluid, magnetic field, Buongiorno model).

An inclined channel was studied by Cimpean and Pop (2012), Aly and Ebaid (2013), Rasekh and Ganji (2013), Sureshkumar and Muthtamilselvan (2016) (moving top lid), and Hayat et al. (2016a, b) (peristalsis, second-order velocity, and thermal slips and Nithyadevi et al. (2017) (heated mid-domain moving wall, sinusoidal heating on a side wall). A horizontal annulus was investigated by Ellahi et al. (2013).

9.7.4.5 Other Cavities

Convection in a lid-driven cavity was studied by Mittal et al. (2013, 2014) Nithyadevi and Rajaarthinam (2015) (cross-diffusion) and Sivasankaran et al. (2016) (two sided drive, partial slip, magnetic field). A problem with various heat source shapes with constant flux in a rectangular horizontal channel was treated numerically by Mahdi et al. (2014). Cavities of various geometrical shapes filled with open cell aluminum foam were studied by Mahdi et al. (2013). Hayat et al. (2016) studied peristalsis of a MHD Jeffery nanofluid in a curved channel.